The Effects of Base-Only-Restrained and Both-Ends-Restrained Conditions on the Ultimate Bearing Capacity of Energy Piles Using Physical Modeling

Mostafa Ebrahimi [1], Mohsen Keramati [1],*, Fahime Rafiee [2], Mohammadreza Moshtaghi [1]

[1] Faculty of Civil Engineering, Shahrood University of Technology, Shahrood, Iran.
[2] School of Engineering, Department of Civil Engineering, Damghan University, Damghan, Iran.

ABSTRACT: Today, ground-source heat pumps (GSHP) are one of the most efficient solutions to reduce energy consumption. Utilizing energy piles as a kind of energy geostructure can enhance the cost-effectiveness of projects incorporating GSHP systems. In this study, the ultimate bearing capacity of an energy pile was compared in the two general base-only-restrained and both-ends-restrained conditions. For each of these two conditions, the relative densities of 48% and 85% and the temperature changes of $\Delta T = 17$ °C and $\Delta T = 30$ °C were regarded as variables. During the test, the soil and pile temperatures, the pile head, the pile tip displacements, and the thermomechanical strains in a pile were recorded. These parameters are used for calculating the temperature profile, thermal stresses of the pile, side shear stresses, and the ultimate bearing capacity of the pile. The results showed that the increase in relative density and temperature led to an increase in thermal stress and ultimate bearing capacity. The minimum UBC increase was obtained for the base-only-restrained condition with a relative density of 48% and $\Delta T = 17$ °C, which was about 10%, while the maximum increase of 21% was obtained for the both-ends-restrained condition with a relative density of 85% and $\Delta T = 30$ °C.

1- Introduction

Heat pumps have low power consumption technology and are the world's leading safe and sustainable heating. Heat pumps on the market are three to five times more efficient than natural gas boilers. GSHP[1] systems are an environmentally friendly solution for supply cooling and heating needs, which work much more efficiently compared to conventional ventilation systems. Using a geothermal heat pump reduces greenhouse gas emissions by 66%, electricity consumption by 75%, and maintenance costs by 75%. In general, it can be said that geothermal heat pumps are the most widely used aspect of geothermal energy, which have the potential to supply energy to communities due to their high efficiency [1, 2]. Energy Piles (which are also named heat exchanger piles or geothermal piles) are used to transfer the superstructure's load to the ground and harvest geothermal energy. The great environmental and economic benefits of using geothermal energy as a renewable energy source have made the use of energy piles popular around the world [3]. Despite the many advantages of using energy piles to harvest shallow geothermal energy, the current energy pile's design heavily depends on experience and empirical rules. The use of high coefficients of safety leads to excessive use of energy and natural resources in the construction and installation of piles, which can be uneconomical and harmful to the environment [4-7].

Several researchers in recent years have presented various numerical and analytical models to analyze energy piles [8-13]. Some others have conducted field-scale studies [14-21]. In very recent studies, [9, 22-24] summarized the discussed available numerical, analytical, and experimental studies and provided critical information regarding the design, construction, and implementation of energy piles. Field-scale tests have several advantages, including considering the real conditions of loading. However, they have limitations, such as high costs, unavailability of a suitable site, and uncertainties in soil and ground conditions that may not allow a comprehensive and accurate understanding of the thermal and mechanical loading process. While, laboratory scale tests, despite the scaling, provide an opportunity for an accurate understanding of the energy pile behavior under fully controlled conditions [22]. Laboratory modeling consistently encounters dimensional constraints; yet, enhanced control over diverse conditions facilitates more precise and less error-prone research. This study involved constructing a model at a scale of approximately 1/6 of the actual piles, adhering to boundary limits and regulatory guidelines. McCartney and Rosenberg analyzed the performance of the modeled energy pile in silt using a centrifuge test. They reported that the side shear capacity increased by 40% when the pile temperature increased from 15 °C to 60 °C [25]. Wu et al.

---

1 Ground Source Heat Pump

*Corresponding author's email: keramati@shahroodut.ac.ir

subjected floating and end-bearing piles to thermal stress, heating/cooling cycles, heating/recovery cycles, and cooling/recovery cycles to stimulate areas with temperature, tropical, and cold climates. They found that pile temperature, soil temperature, and pore water pressure were almost balanced in a temperate climate. However, pile and soil temperatures would not stabilize during thermal cycles in tropical and cold climates. The values of irreversible displacement due to five thermal cycles for temperate, tropical, and cold climates were reported to be 0.67%D (D is the pile diameter), 0.47%D, and 0.26%D, respectively [26]. Pasten and Santamarina also reached similar conclusions about irreversible displacements after several thermal cycles [27]. Ng et al. modeled a pile in saturated sand in the centrifuge experiment. They reported a 1.4%D heaved in the pile head initially when 30 °C increased the pile temperature, but when the temperature stabilized, this value reduced to 0.8%D after four months. The bearing capacity of the pile also increased by 13% and 30% when the temperature was raised by 15 °C and 30 °C, respectively [28]. Apart from the centrifugal experiment, some other researchers used a 1-g physical model to analyze the thermal and thermomechanical performance of the energy pile. Ghasemi-Fare and Basu analyzed the behavior of an energy pile installed in dry and saturated sand and concluded that the temperature near the pile increased more under dry conditions. However, the temperature increase was more significant at a farther distance from the pile in saturated soil since saturated soil facilities the heat transfer mechanism in the soil medium. In addition, thermal insulation at the soil surface affected the efficiency of the geothermal pile for a short time after the onset of thermal loading [29, 30]. Kramer and Basu that performed a similar test, concluded that the bearing capacity increases by about 5.5% when the pile temperature rises from 20 °C to 40 °C [31]. Goode and McCartney modeled floating piles and an end-bearing base with both-ends-restrained conditions in a centrifuge test in dry sand and unsaturated silt. They concluded that an increase in temperature increased the bearing capacity of unsaturated silt, while it had little effect on dry sand. They also pointed out that the thermal axial stress increased in both-ends-restrained conditions compared to the base-only-restrained condition [32]. Liu et al. tested two piles with U-shaped and W-shaped heat exchangers in dry and saturated sand under one, three, and five heating-cooling cycles. They concluded that increasing the pile's temperature increased its bearing capacity. However, the bearing capacity decreased after the cooling cycles. The decrease in bearing capacity after three and five cooling cycles was 13.4% and 9.2%, respectively. They also concluded that the method of compaction (or relative density) has important effects on the bearing capacity [33]. Sutman et al. conducted a study in Richmond, Texas (US), with full-scale field tests on three geothermal piles, two of which were placed on an end-bearing base (the first pile was thermally loaded only, and the other piles were thermomechanically loaded) to evaluate the thermomechanical behavior of the energy piles. The results showed that the compressive stress in an energy pile with thermomechanical loading was higher than in a thermally loaded pile. The thermal resistance of the side changed its direction more with thermomechanical loading than solely with thermal loading [34, 35]. In another study, Senjani et al. modeled a pile in dry sand and concluded that reversible settlements occur when the load is less than 20% of the bearing capacity of the geothermal pile, but that irreversible displacement occurs when they exceed this value [36]. Despite many studies performed on analyzing the load transfer mechanism in energy piles under thermomechanical loading, only a few studies repeat the same experiments with only varying the boundary conditions at the pile head and pile base to analyze the role of relative density on the thermomechanical stress along the pile under variable pile head and base conditions. This study investigated different conditions for energy piles using physical models. The main objective of this study was to evaluate the effects of temperature variation and relative density on the ultimate bearing capacity of energy piles in two base-only-restrained and both-ends-restrained conditions.

The particular innovation of this research is that, despite the studies conducted to study the thermomechanical performance of energy piles, there are still many uncertainties and discrepancies in research findings. One of the most effective conditions of the thermomechanical performance of the pile is the head and base condition. The semi-floating condition for energy pile is investigated in [37, 38], but the end-bearing condition, which means the pile base sitting on an incompressible bedrock and also both ends restrained condition which on that base and head of the pile grip and limited. Testing on a laboratory scale can provide a proper understanding of the behavior of energy piles in controlled conditions. Only now, several researchers have modeled energy piles on a large scale in the laboratory. However, they have yet to investigate the thermomechanical behavior of the pile under different thermal loads and various pile head and base stiffness. This study investigates the thermomechanical behavior of the pile under two different stiffness conditions, base-only-restrained and both-ends-restrained, of the energy pile in 48% and 85% relative densities of dry Firoozkooh sand and the effect of temperature changes of $\Delta T=17$ °C and $\Delta T=30$ °C on the stress and ultimate bearing capacity.

When the bedrock is close to the ground surface, engineers and designers are more inclined to implement piles for the foundation of structures than by placing piles on incompressible bedrock. The forces of the upper structure are transferred to the bedrock, which has a very high bearing capacity, instead of the soil. In the research related to energy piles, more studies have been done in the semi-floating condition; therefore, it seems necessary to conduct more studies on the end-bearing condition of energy piles.

2- Materials and methods

In this modeling, there were four main phases, which include: heat exchanger fluid, fluid transfer pipes, concrete, and soil. For the heat exchanger fluid in this test, pure water was used, and its characteristics are known to the researchers. The specifications of other materials are described below.

Table 1. Soil Properties

Parameter	Value	Unit
USCS (Soil Name)	SP	-
D_{10}	0.76	mm
D_{50}	1.318	mm
C_c	1.061	-
C_u	1.889	-
Gs	2.65	-
e_{max}	0.96	-
e_{min}	0.66	-
$\gamma_{d\,max}$	15690.64	N/m^3
$\gamma_{d\,min}$	13238.97	N/m^3
γ_d (Dr = 48%)	14317.70	N/m^3
γ_d (Dr = 85%)	15298.37	N/m^3
λ_g (thermal conductivity)	0.35	W/m.K
C_{ps} (Specific heat)	≈ 850	J/kg.K
ρc (Volumetric heat capacity)	≈ 1150000	J/m^3.K
υ_g (poisson's ratio)	0.3	-
φ (Dr = 48%)	$31.57 \approx 31.6$	°
φ (Dr = 85%)	$37.96 \approx 38$	°
C (Dr = 48%)	$0.69 \approx 0$	kPa
C (Dr = 85%)	$4.26 \approx 0$	kPa

2- 1- Soil Specifications

This study used D11 Firoozkooh sand to fill the soil box with approximately relative densities (Dr) of 48% and 85%. In this modeling, due to the moving of the box, it is very difficult to keep the percentage of relative density very accurate, and by measuring the changes in the level of the soil, it was found that the relative density in each test has about 2% error probability, that is the reason, the percentage of relative density is displayed with an approximate sign. Of course, this error percentage can be completely ignored according to the obtained results.

The sand's highest and lowest dry densities are 15.69 and 13.23 kPa, respectively. Table 1 presents the properties of the soil used in this research. As you can see in Table 1, the sand is composed of uniform, angular particles, which are of the "poorly graded" type (SP) according to the Unified Soil Classification System (USCS). The internal friction angles for the relative densities of 48% and 85% were 31.6 and 38 degrees, respectively, and the cohesion was approximately zero at both relative densities due to the dryness of the sand.

Influential parameters in software modeling for energy piles are soil cohesion (C) values and friction angle (ϕ). A Triaxial test based on ASTM D4767-11 has accurately measured these values. Figures 1 and 2 show the diagram of soil Mohr's circles for two different relative densities tested in this modeling.

2- 2- Pile model and soil tank

A precast concrete pile with a diameter of 10.5 cm, a length of 100 cm, and a buried depth of 92 cm was installed in the soil box. A U-shaped polyvinyl chloride (PVC) flow pipe with inner and outer diameters of 16 and 20 mm is embedded inside the modeled pile for hot water circulation. Each branch of the U-shaped pipe is located 27 mm from the pile's center. As shown in Fig. 3, the heat exchanger pipes were connected to a temperature-controlled flow circulation tank (water bath) to control the fluid inlet temperature. The water temperature at the inlet and outlet points was recorded during the tests.

2- 3- Concrete specification

The concrete mix design was selected according to FHWA regulations. The elastic modulus at 28 days after pile construction was determined to be 29,700 MPa. The concrete mixture of the piles was designed using 10.4%: 24.52%: 31.53%: 33.55% of water, cement, coarse aggregate, and fine aggregate by weight percentage ratio, respectively.

The energy pile was modeled in a physical modeling box with length, width, and height of 127, 100, and 120 cm, respectively, as shown in Fig. 3. More details about the loading process and the system can be found in [39, 40]. More detail on the materials used in this modeling and the material identification test resultss result is presented in [37, 41, 42].
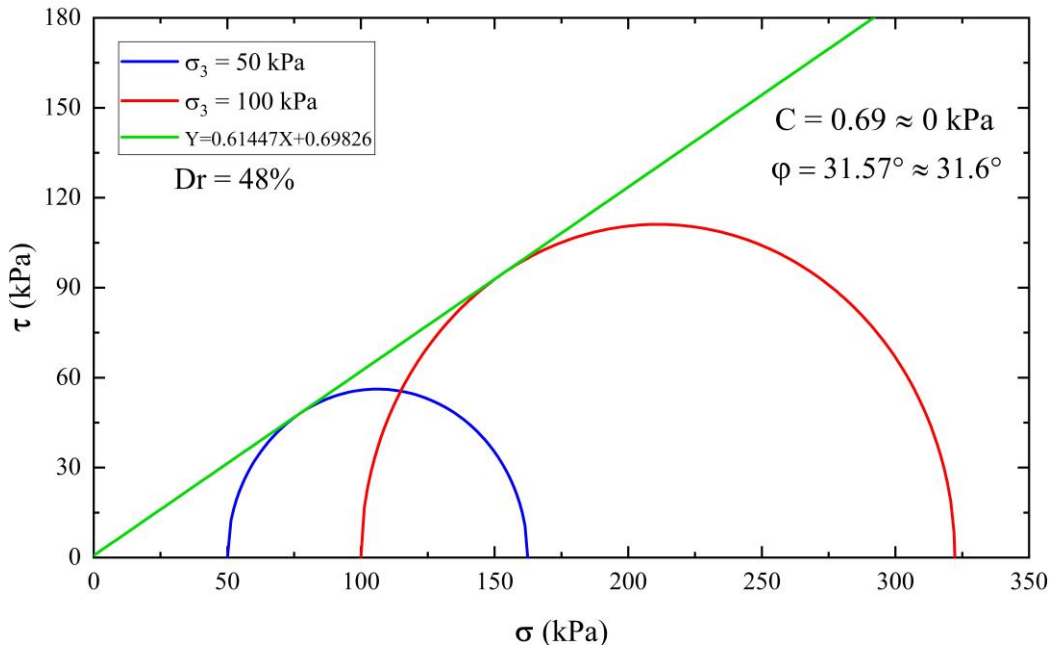
Fig. 1. Mohr's Circles of D11 Firoozkooh sand in triaxial test for Dr = 48%
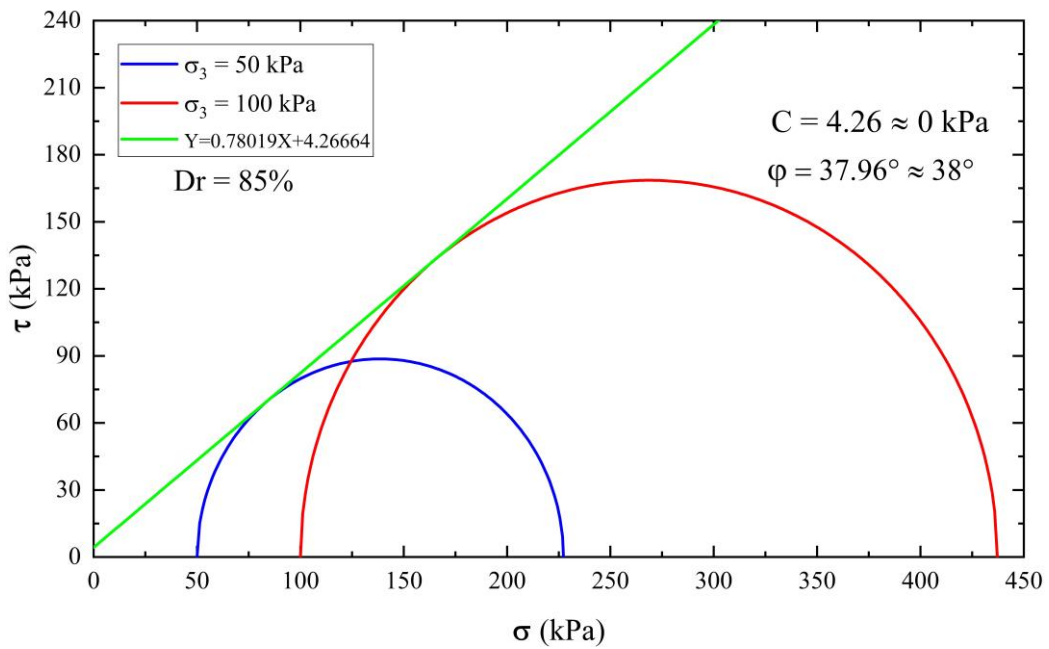

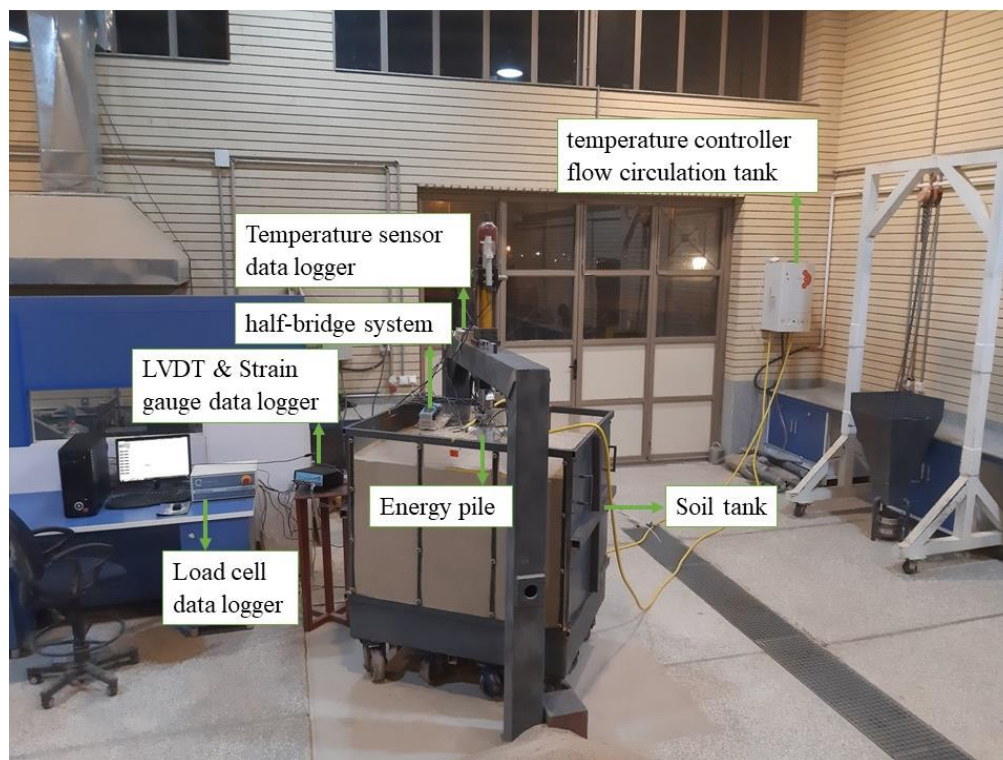**Fig. 2. Mohr's Circles of D11 Firoozkooh sand in triaxial test for Dr = 85%**

Fig. 3. Modeling overview

3- Test Configuration

The required soil weight for each test was calculated to fill the modeling box with the target relative density, with the soil characteristics (γ_{dmax} and γ_{dmin}) and using Eq. (1). While filling the box layer by layer, the pile base (concrete base for end-bearing model), energy pile, and temperature sensors were placed in the designated place (base on Fig. 5). Then with the completion of the construction of each test, the required sensors on the pile were connected to the pile head.

$$Dr = \frac{(1/\gamma_{d\min}) - (1/\gamma_d)}{(1/\gamma_{d\min}) - (1/\gamma_{d\max})} \tag{1}$$

The mechanical load was measured during the tests using a load cell with a 98 kN capacity. Two LVDTs were installed to measure the pile head and base displacements. A steel rod was attached to the bottom plate of the pile, and a small tube was placed around it to prevent contact with the pile concrete. Then an LVDT was placed on a plate connected to the top of the rod to measure the pile base's displacement without affecting the pile's compression. Another LVDT was placed on the pile plate to measure the pile head's displacement. The Load cell and the LVDTs installed at the pile head and base are shown in Fig. 4a. The view of the assembled test is shown in Fig. 3.

Goode and McCartney used a cylindrical aluminum tank to model the end-bearing condition and concluded that this caused heat exchange with the outside of the box through the soil [32]. However, in this study, a concrete cylinder with a diameter of 15 cm and a height of 24 cm was used on the base of the soil tank for modeling end-bearing conditions. Then, the pile was placed on it to prevent heat exchange with ambient temperature from the bottom of the box, as shown in Fig. 4b.

A total of 50 temperature sensors were placed inside the box to measure the soil and pile temperatures, the temperature at the edge of the box, room temperature fluctuations (if there were any), and the inlet and outlet temperatures. Figure 5 presents the location of the temperature sensors installed in a plane passing the heat exchanger tubes. Furthermore, several thermocouples were placed in the plane perpendicular to the U-shaped heat exchanger piles. In addition, seven sensors were placed along the edge of the box to monitor the temperature evolution inside the soil and to stop the thermal loading once the heat reached the soil box boundaries and the heat transfer between the box and the environment was established. For measuring the temperatures, the DS18B20 Temperature Sensor with an accuracy of ± 0.5 °C was used, and this sensor was connected to a data logger with a rate of 1 Hz. For harvest strain data, a data logger with the rate of 100 kHz and 8-channel was used; for LVDT data also used this data logger. The load cell was connected to a 16-channel
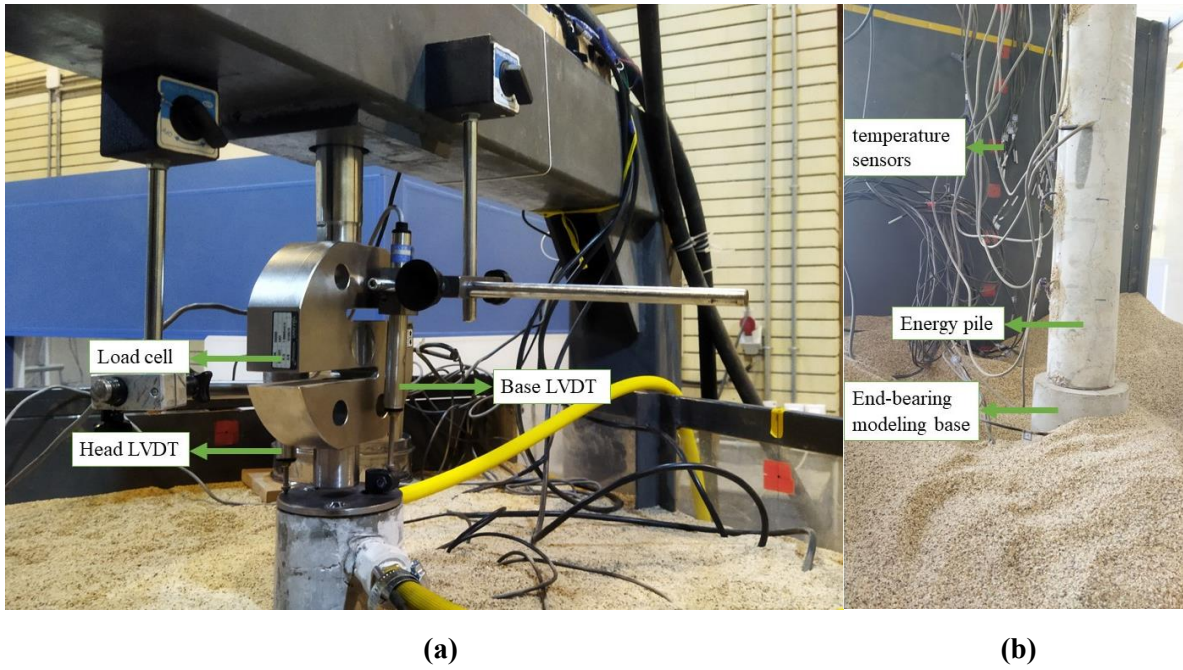
(a) **(b)**

Fig. 4. A view of the equipment (a) Details of the test set-up on the head of the pile, and (b) The inside view of the box and end-bearing modeling base.
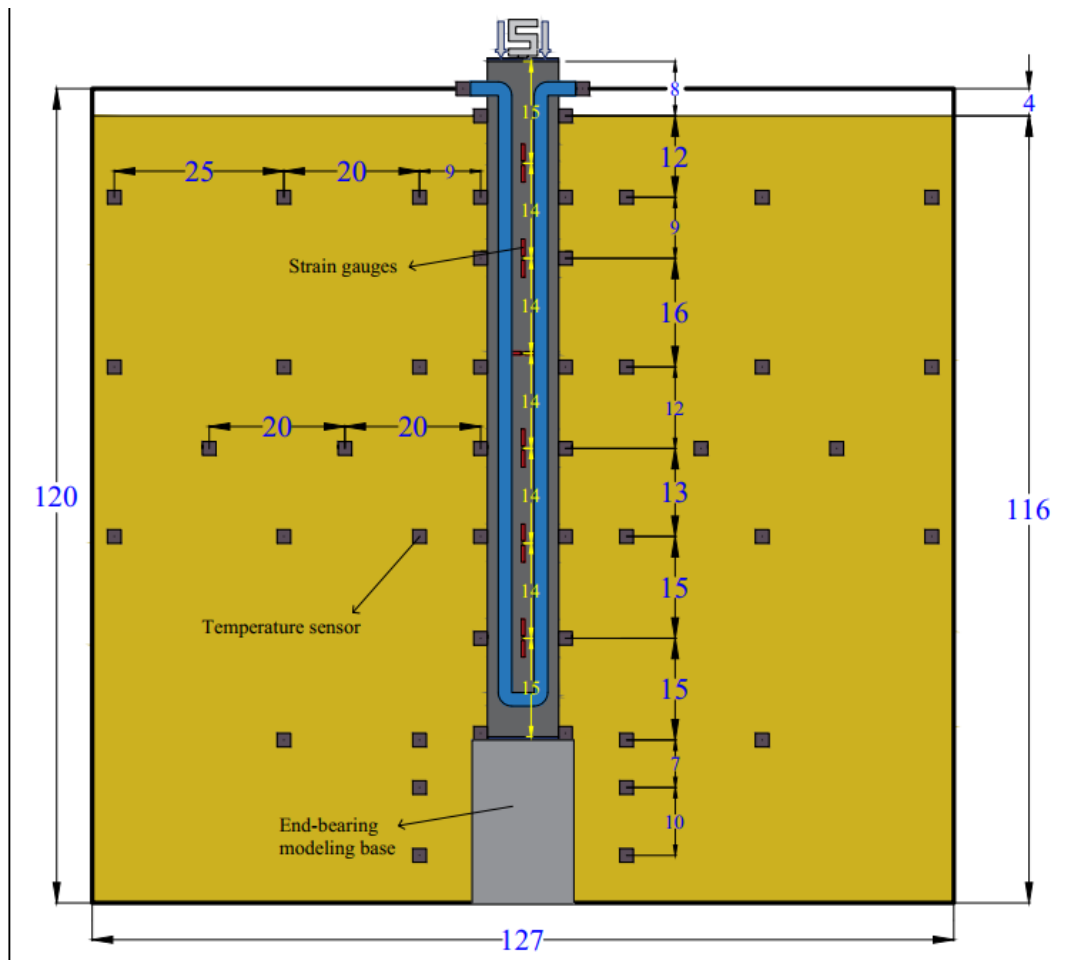

Fig. 5. Schematic view of the sensor's locations.

Table 2. Tests detail.

Test name	Pile type [a]	Relative density $\approx$ (%)	Thermal load	ΔT (°C)
Test 1	EP-E	48	No	-
Test 2	EP-E	85	No	-
Test 3	EP-E	48	Yes	+17
Test 4	EP-E	48	Yes	+30
Test 5	EP-E	85	Yes	+17
Test 6	EP-E	85	Yes	+30
Test 7	EP-B	48	Yes	+17
Test 8	EP-B	48	Yes	+30
Test 9	EP-B	85	Yes	+17
Test 10	EP-B	85	Yes	+30

[a] EP-E end-bearing energy pile, EP-B both ends restrained energy pile.

dynamic data logger with a rate of 200 kHz. By conducting calibration tests, it was found that the strain sensors have a maximum error of 2%, which is very suitable for doing this modeling.

To model the end-bearing conditions, the pile was sitting on the concrete cylinder shown in Fig. 4b, and in addition, for the both-ends-restrained condition, the pile head was connected to the hydraulic loading jack to limit the upward movement of the pile.

To measure the strains developed in a pile under mechanical, thermal, and thermomechanical loading, 12 strain gauges were attached at six different depths along the pile. The half-bridge system (two strain gauges facing each other) was used to avoid errors due to temperature increase. Considering the half-bridge method reduces the error of the thermal strain to around 2% to 3%, Ten strain gauges from those mentioned earlier were installed in line with the pile, and two stain gauges were installed perpendicular to the pile for measurement of radial strain, but unfortunately, they were damaged during the test and did not record any data. The damaged strain gauge does not have any effect since with the remaining 5 strain gauges, the process of force distribution in the pile can be clearly investigated.

3- 1- Testing procedure

After installing the model energy pile with an end-bearing base, the soil box was filled with sand with the desired relative density. The box was filled layer by layer (each layer height is about 25 cm) by calculating the amount of soil weight needed to reach the desired relative density; more detail about filling the box is presented in [37]. At each specific layer, the temperature sensors were embedded in the soil. For each relative density, a mechanical load of 3.432 kN was loaded on the pile in a load-controlled condition at a constant rate of 0.49 kN/min and unloaded at the same rate after loading. Thermal

loading was applied by keeping the inlet pile temperature constant. Two initial temperature gradients of 17 °C and 30 °C at the inlet point were imposed during the experiment, and the thermal loading was continued until the heat reached the sides of the soil box. After that, the heat exchanged with the environment, and the soil temperature was stable. Mechanical loading and unloading were performed when the pile and the pile-soil interface temperature were stabilized.

A total of 10 tests were conducted on the modeled pile under the base-only-restrained and both-ends-restrained conditions. The details of the relative density and temperature of each test are summarized in Table 2.

For modeling the end-bearing condition, as mentioned before, the pile was put on concrete cylindrical as an incompletion bedrock, and for both ends, restrained condition; besides that, the head of the pile was also fixed and limited for lateral displacement.

4- Result and disscusion

As mentioned earlier, the inlet temperature was kept constant for almost five days until the temperature of the boundary increased by 1 °C. During these five days, the soil temperature surrounding the modeled energy pile reached equilibrium. Figure 6a shows the initial temperature profile of the soil just before starting the test. Figures 6b and c show the soil temperature at the end of 5 days, respectively, for the base-only-restrained condition and the both-ends-restrained with a relative density of 48% and ΔT = 17 °C and 30 °C. Although it is expected that the concrete cylinder used to model the end bearing condition would not change the thermal response of the soil, a comparison of Fig. 6b and c can determine whether the mechanical boundary condition had any effect on the soil temperature.

Additionally, comparing Figures 6b and c indicate the increase in soil temperature when the thermal gradient
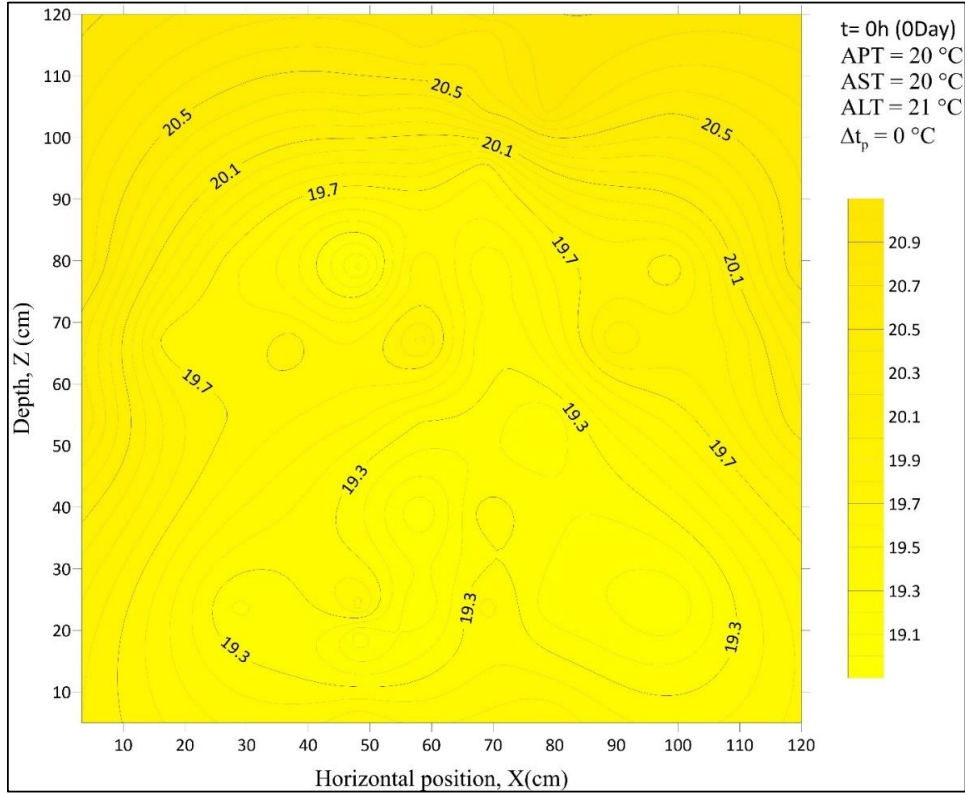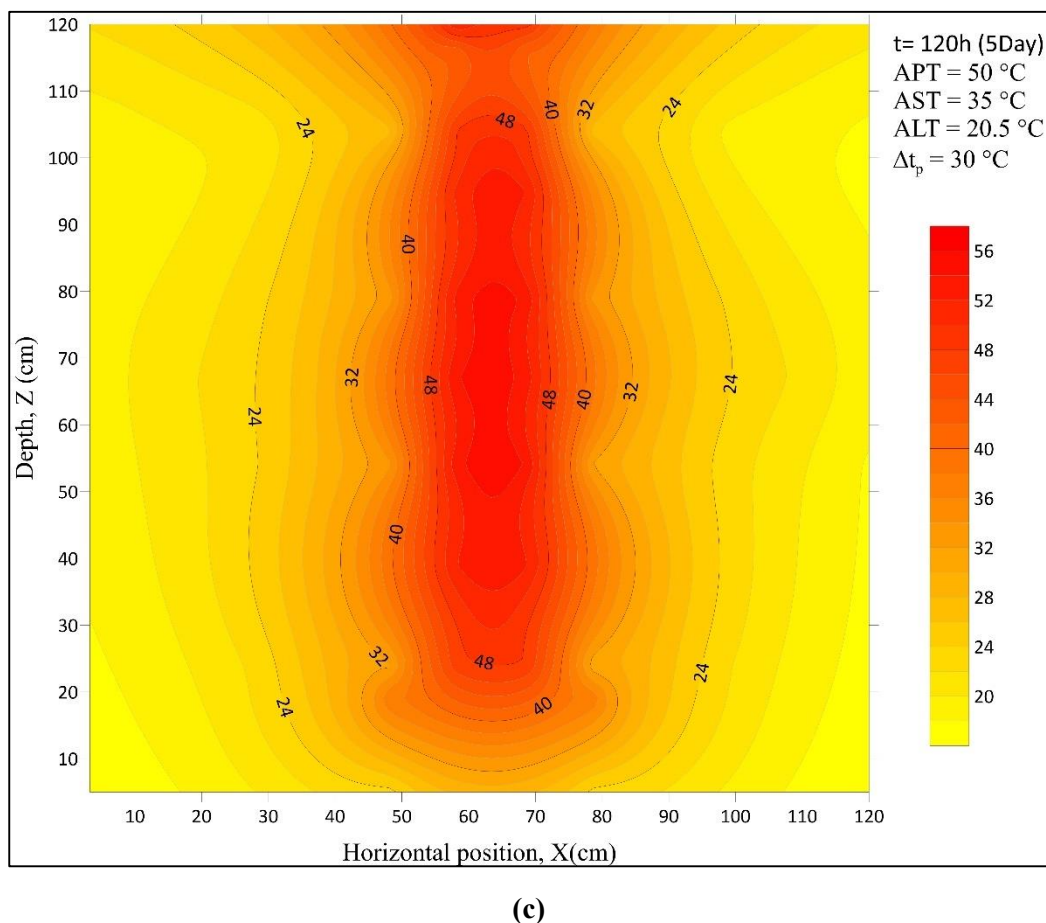
(a)
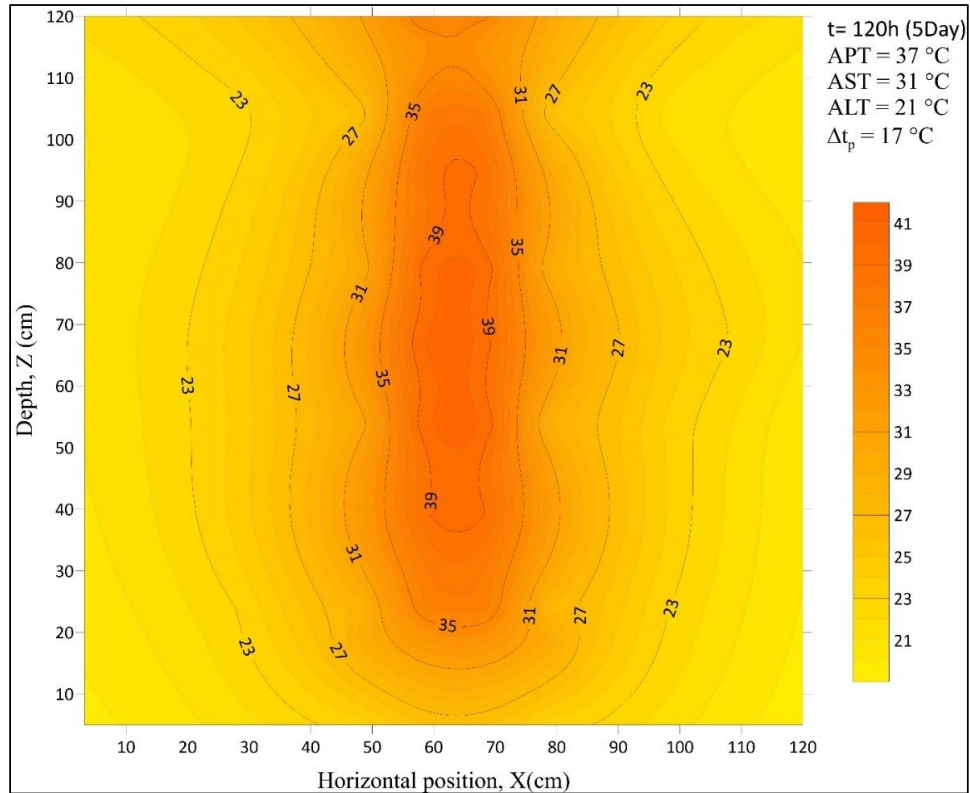
(b)

Fig. 6. The temperature profile of the soil in different thermal loads: (a) before thermal loading started, (b) after 5 days with ΔT= 17 $^\circ$C, and (c) after 5 days with ΔT= 30 $^\circ$C. [APT = Average pile temperature, AST = Average soil temperature, ALT = Average lab temperature, ΔTp = Change in pile temperature.(Continued)

(c)

Fig. 6. The temperature profile of the soil in different thermal loads: (a) before thermal loading started, (b) after 5 days with ΔT= 17 °C, and (c) after 5 days with ΔT= 30 °C. [APT = Average pile temperature, AST = Average soil temperature, ALT = Average lab temperature, ΔTp = Change in pile temperature.

almost doubles. Please note that the current study focuses on analyzing the thermomechanical response of an energy pile. Despite recorded temperature data for all tests, only three soil temperature profiles are presented here.

Figure 7 shows the axial load versus pile settlement at three different temperatures for 48% and 85% relative densities. In all tests, the mechanical loading is applied at a constant rate of 0.49 kN/min until it reaches 3.432 kN. Due to the end grip of the pile, where the pile is placed on the incompressible bedrock, the pile's settlement due to mechanical loading is very small (maximum 0.6 mm), which is a large percentage of this settlement caused by the contraction of the pile. After conducting these tests, it was found that increasing the pile's temperature reduced the pile head displacement when the temperature increased to ΔT= 17 °C at a relative density of 48%, and the settlement decreased by 20% at the limit state condition. In comparison, when ΔT= 30 °C, the settlement decreased by 30%. However, thermal loading of ΔT= 17 °C and ΔT = 30 °C at a relative density of 85% reduced the pile settlement by 19% and 30%, respectively. This can be caused by increasing the interaction between soil and pile, expansion

of the pile, or moving up the upper section of the pile, all due to increasing the temperature. Naturally, as the temperature increases, the expansion created in the pile increases, and the settlement decreases more.

To confirm the truth of this issue, it can be mentioned that Liu et al. [33], Goode and McCartney [32], and Ahmadipour and Basu [43] also showed that pile head settlement decreased when pile temperature increased. Liu et al. discussed that the reduction in pile head settlement is due to the thermal expansion of the pile. Since the thermal expansion coefficients of soil and concrete are not significantly different, they explained that the difference in expansion was due to the temperature distribution from the pile to the soil. However, if the pile and the soil expand at the same rate, the stress does not change [33].

Equation (2) and (3) were used to calculate the mechanical and thermal stress using the mechanical and thermal strain data [44].

$$\sigma_M = E \varepsilon_M \qquad (2)$$

169
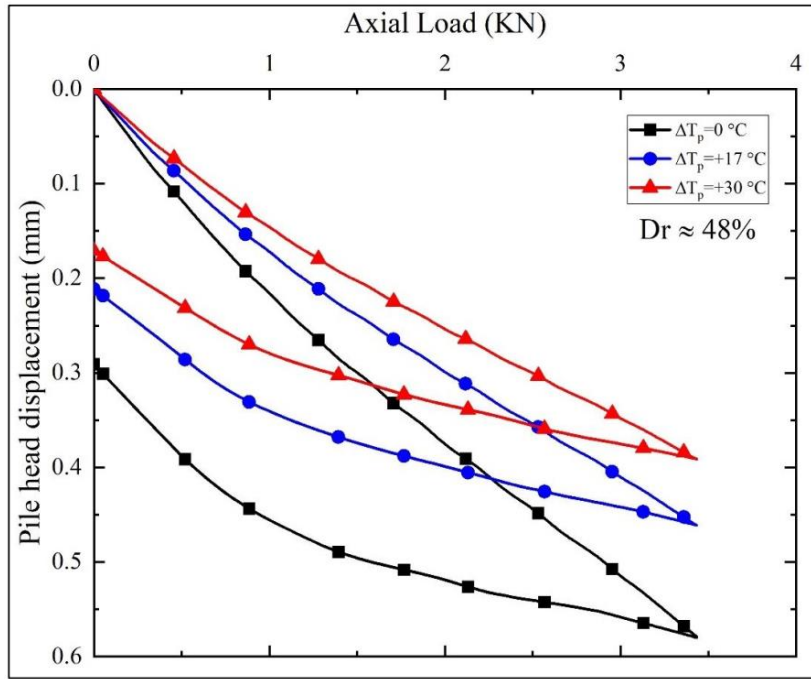
(a)
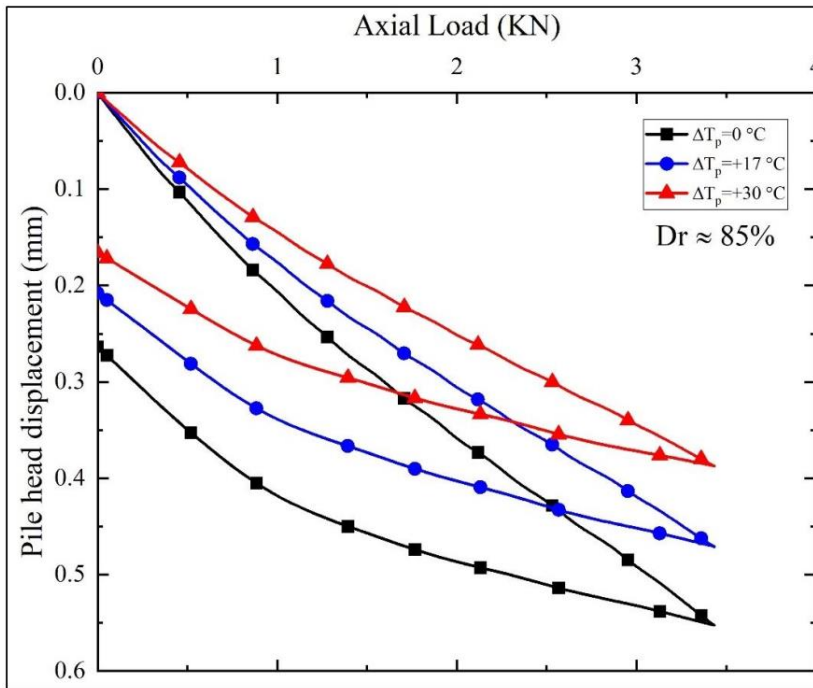
(b)

Fig. 7. Axial load versus settlement at different temperatures, (a) relative density of 48%, (b) relative density of 85%.

$$\sigma_T = E(\varepsilon_T - \alpha_c \Delta T) \qquad (3)$$

Where σ_M is the mechanical stress, E is the modulus of elasticity, ε_M is the mechanical strain, σ_T is the thermal stress, ε_T is the thermal strain, ΔT is the temperature change, and α_c is the coefficient of thermal expansion, which is equal to 10^{-5} 1/°C.

The mechanical, thermal, and thermomechanical stress induced in a pile is presented in Fig. 8a, b, and c. Figure 8a shows the mechanical stress distribution along the depth for the both-ends-restrained condition with 48% and 85% relative densities. In mechanical loading only, due to the limited movement of the pile at both ends, the amount of stress created along the length of the pile is almost equal at all points, which was expected. The amount of stress is almost the same at these two relative densities. However, the increase in relative density has slightly reduced the stress level. Figure 8b shows the stress induced by the thermal load for the both-ends-restrained condition with the two relative densities of 48% and 85%. As seen in the that, the thermal stress has significantly increased for higher thermal loading. One of the important results that can be understood from this graph is

that the effect of temperature is significantly greater than the effect of relative density. This means that the amount of stress generated in the energy pile depends on the temperature of the ground and the pile, and it is necessary to pay attention to the temperature parameter in the designs.

Figure 8c illustrates the changes in thermomechanical stress along the modeled energy pile in both-ends-restrained conditions. Like thermal stress, thermomechanical stress increases due to increasing the temperature and relative density. The values of thermomechanical stress are almost equal to the sum of mechanical and thermal stress.

Figure 9 demonstrates the thermal and thermomechanical stress along the depth in the two base-only-restrained and both-ends-restrained conditions with two different relative densities. As seen in Fig. 9a, the pile head and base stresses are almost identical in both-ends-restrained conditions. Figures 9a and b show the thermal stresses in the two base-only-restrained and both-ends-restrained conditions in 48% and 85% relative density. As Fig. 9a shows, an increase in temperature from $\Delta T= 17$ °C to $\Delta T= 30$ °C increased the thermal stress for base-only-restrained and both-ends-restrained conditions by 71% and 63%, respectively, at 48% relative density. In addition, a higher increase in thermal
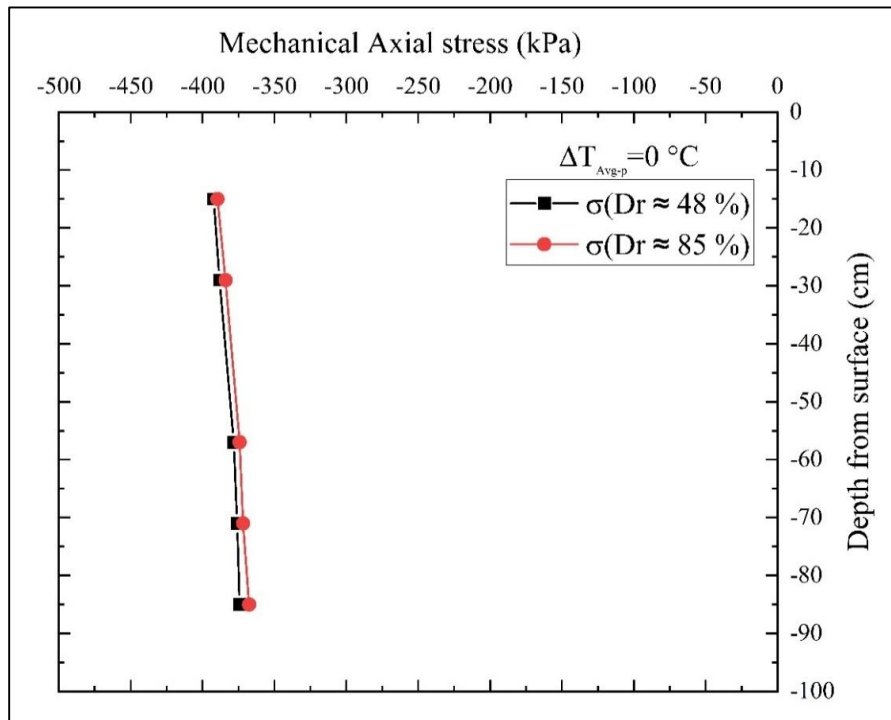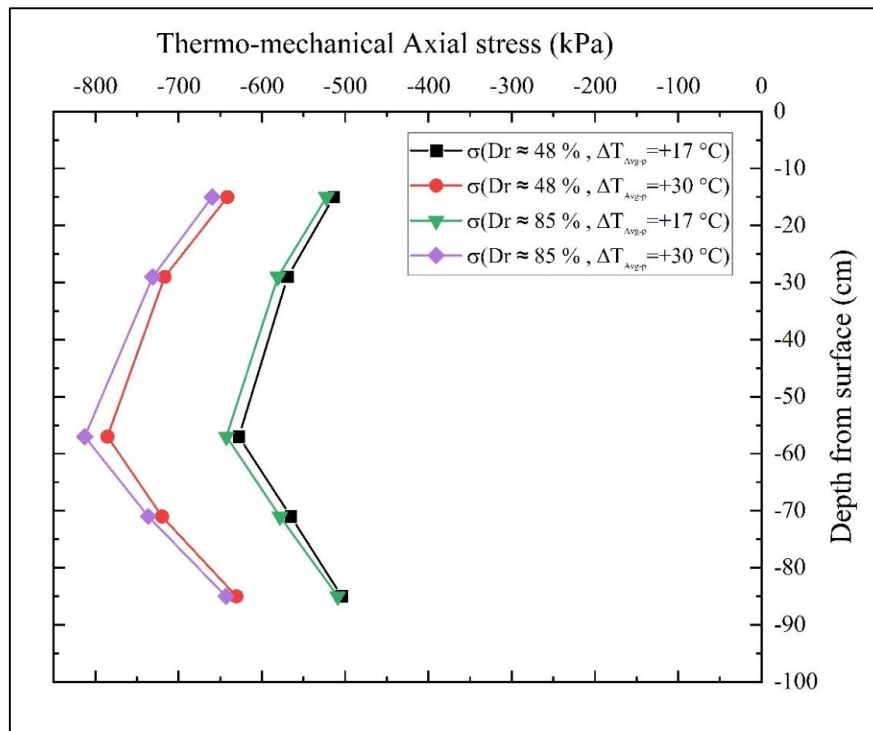

(a)

Fig. 8. Stress distribution along the depth in the both-ends-restrained condition, (a) mechanical stress, (b) thermal stress, and (c) thermomechanical stress.(Continued)
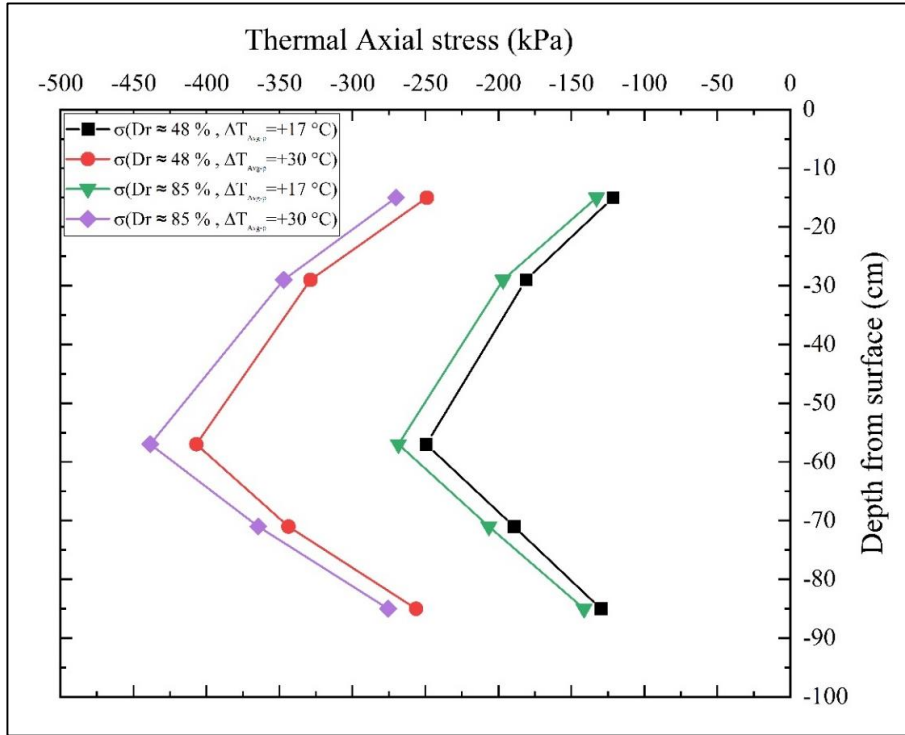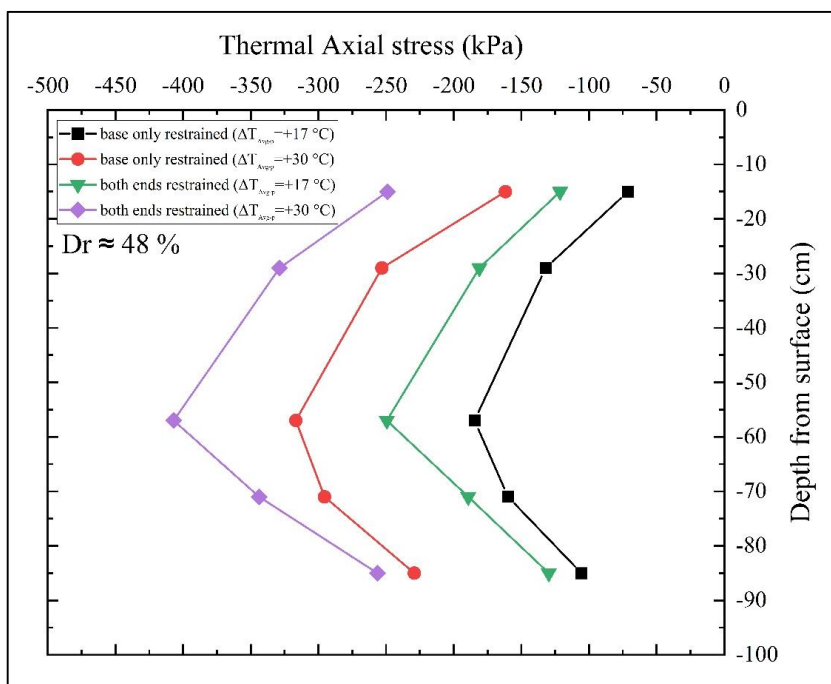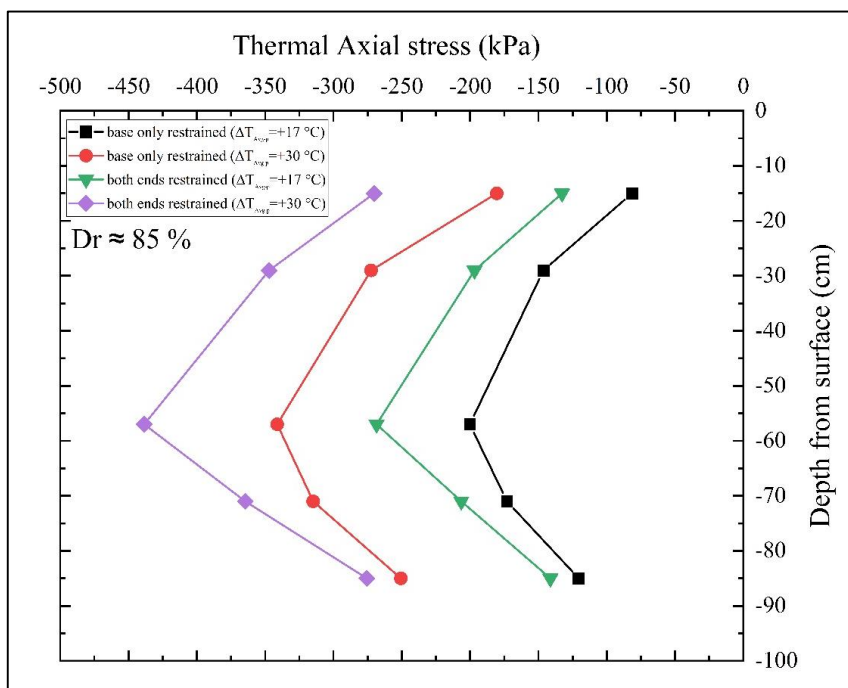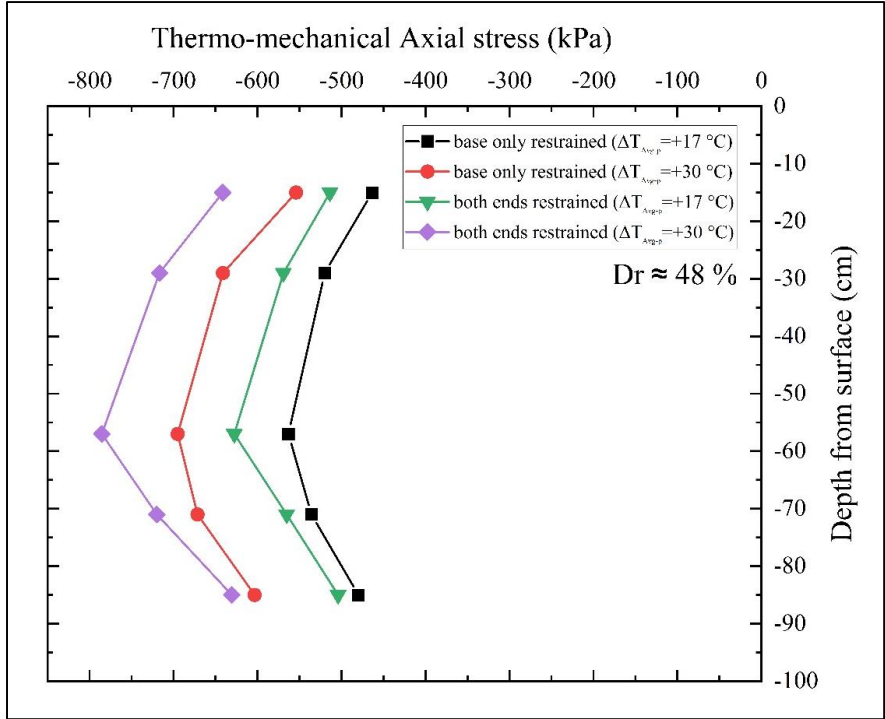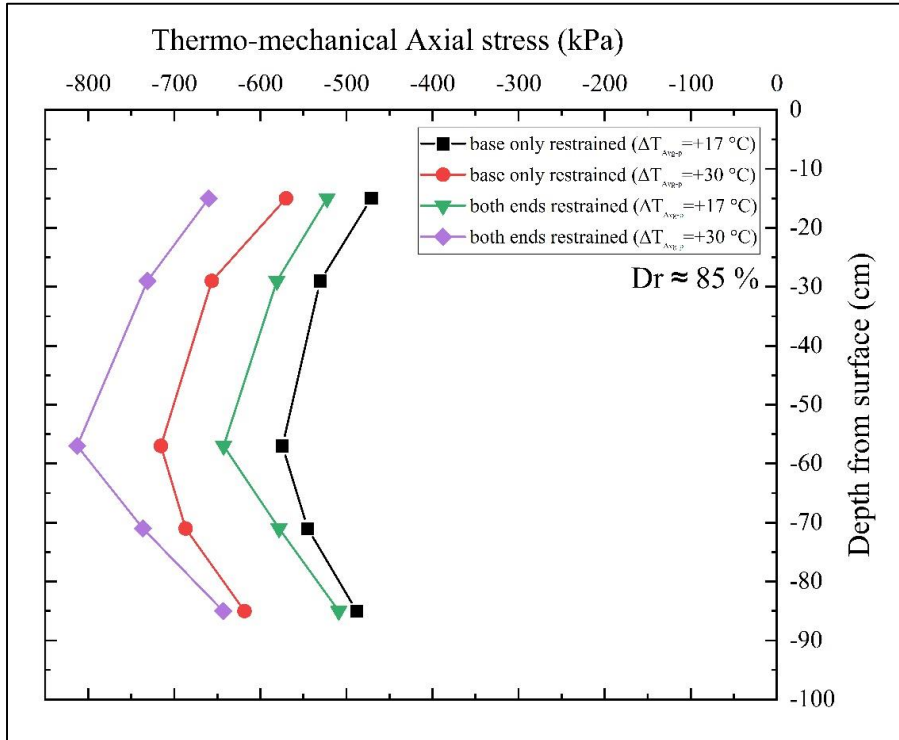
(b)

(c)

Fig. 8. Stress distribution along the depth in the both-ends-restrained condition, (a) mechanical stress, (b) thermal stress, and (c) thermomechanical stress.

(a)

(b)

Fig. 9. Stress versus depth in two base-only-restrained and both-ends-restrained conditions: (a) thermal stress with a relative density of 48%, (b) thermal stress with a relative density of 85%, (c) thermomechanical stress with a relative density of 48%, and (d) thermomechanical stress with the relative density of 85%.(Continued)

(c)

(d)

Fig. 9. Stress distribution along the depth in the both-ends-restrained condition, (a) mechanical stress, (b) thermal Stress versus depth in two base-only-restrained and both-ends-restrained conditions: (a) thermal stress with a relative density of 48%, (b) thermal stress with a relative density of 85%, (c) thermomechanical stress with a relative density of 48%, and (d) thermomechanical stress with the relative density of 85%

stress was observed in the both-ends-restrained condition than in the base-only-restrained condition. For the latter case, 35% and 28% increase in thermal stress were observed, respectively, for ΔT = 17 °C, ΔT = 30 °C. Furthermore, Fig. 9b presents the thermal stress at a relative density of 85%, which is almost the same as the thermal stress at Dr = 48%.

Figure 9c and d show the thermomechanical stresses in the 48% and 85% relative densities for the base-only-restrained and both-ends-restrained conditions. As can be seen, the thermomechanical stresses have increased similarly to the thermal stresses. An increase in temperature results in higher stress. Additionally, the stresses are higher in the both-ends-restrained condition than in the base-only-restrained condition.

According to the comparison of the end-bearing and both-ends-restrained states in the diagrams of Fig. 9, it is clear that by limiting the pile head displacement, the stress values in the pile increase. In other words, it can be acknowledged that among the different conditions of the pile, i.e., semi-floating, end-bearing, and both-ends-restrained, the both-ends-restrained state generated the highest stress in the pile, and the semi-floating state generated the least stress.

As shown in Fig. 8 and 9, thermal loading and subsequent thermal expansion have increased thermal stresses. In addition, thermal loading changes the stress and stress distribution in the both-ends-restrained condition, and higher thermal stresses were observed in the both-ends-restrained condition, similar to the result announced by [32, 34].

Side shear stress was calculated from Eq. (4) for mechanical, thermal, and thermomechanical loads [45].

$$f_s = \frac{\Delta\sigma \times D}{4\Delta l} \qquad (4)$$

Where f_s (kPa) is the side shear stress, $\Delta\sigma$ (kPa) is the difference between the stresses obtained between two consecutive strain gauges, D (cm) is the diameter of the pile, and Δl (cm) is the distance between the two strain gauges placed on the pile.

The side shear stress was calculated for all tests using Eq. (4), considering both mechanical and thermal stresses. Figure 10 shows the side shear stress for the two relative densities and the different temperatures in the base-only-restrained condition. Figure 11 shows the side shear stress for all variables in the both-ends-restrained condition. The lower amount of side shear stress in mechanical only stress in Fig. 10 and 11 confirms that the modeled energy pile is an end-bearing pile, and the pile base carries most of the load under mechanical loading. The values of the shear stress created on the pile side are used to calculate the bearing capacity of the pile. It should also be noted that in the shear stress diagrams, wherever the stress value changes sign (from negative to positive), it shows the location of the null point, and it is where the amount of strain is zero.

Sutman et al. stated that the both-ends-restrained condition has two main effects on side shear stress: First, the depth at which the shear stress changes its direction due to the increased temperature is extended towards the pile head, whereas in the base-only-restrained condition, it is extended upwards because the pile head is free [34]. This can also be seen in Fig. 10 and 11. Secondly, the side shear stress in the both-ends-restrained condition is lower than in the base-only-restrained condition. The reason is that the pile head is free in the latter condition, which leads to greater axial displacement relative to the surrounding soil. This behavior is evident in the present study.

The bearing capacity of the pile was calculated for all the tests. The method of calculating the bearing capacity of the pile using shaft resistance is given in [37]. Figure 12 illustrates the pile base and shaft resistance versus the pile head settlement for the two base-only-restrained and both-ends-restrained conditions. As shown, due to the existence of the end-bearing modeling base at the pile base, only a small portion of the total load capacity is carried by the pile shaft resistance, and most of the load is carried by the pile base resistance. In addition, the bearing capacity is increased, and pile head settlement is decreased at higher thermal loading in all tests.

The rise in bearing capacity at higher temperatures can be attributed to the increase in base resistance, shaft resistance, or both [43]. Various factors may play a role in such an increase in base and shaft resistances. Pile expansion may have increased lateral restraint at the soil-pile interface [12, 46, 47]. In thermal loading only, the bearing capacity of the pile increases in most cases, both in this study and in previous studies, but when the loading is in the form of cooling-heating cycles, the result can be different.

Figure 13a illustrates the exact value of the base and shaft resistance obtained for all tests separately, and Fig. 13b shows the sum of the base and shaft resistance values (the ultimate bearing capacity) for all tests. As mentioned before, the value of ultimate bearing capacity was increased, which the amount of it is shown in Fig. 13.

As shown in Fig. 13b, the ultimate bearing capacity increased at a higher temperature. For the base-only-restrained condition at the relative density of 48%, it was increasing the temperature from ΔT = 0 °C to ΔT=17 °C (Test 3) and from ΔT=17 °C to ΔT=30 °C (Test 4) increased the ultimate bearing capacity by 10% and 13%, respectively, compared to the solely mechanical load (Test 1). These changes in Test 7 and Test 8, both ends restrained condition with a relative density of 48%, were measured at 11% and 16%, respectively, compared to Test 1. In the test with the relative density of 85% and ΔT=17 °C (test 5), the ultimate bearing capacity increased by 14% compared to the test under the only mechanical load (Test 2), while it was 19% with the same relative density and ΔT=30 °C (Test 6). However, in Test 9 and Test 10 (both ends restrained condition with a relative density of 85%), the ultimate bearing capacity increased by 15% and 21%, respectively, compared to Test 2. The values for the increase in bearing capacity are summarized in Table 3.

Figure 14 shows the changes in bearing capacity under different thermal loads in sand obtained in different studies.
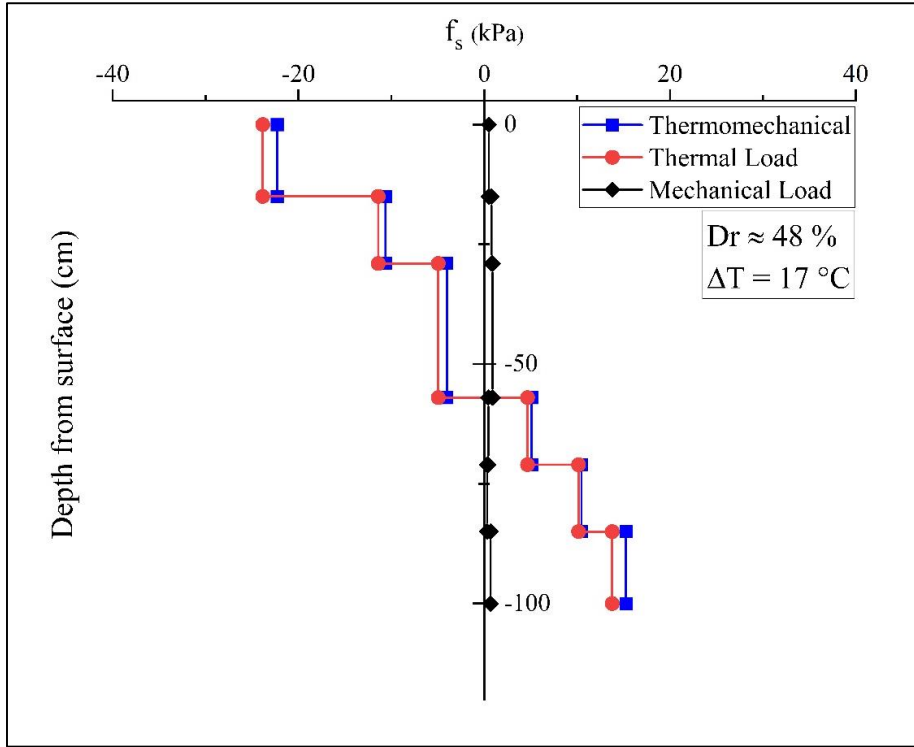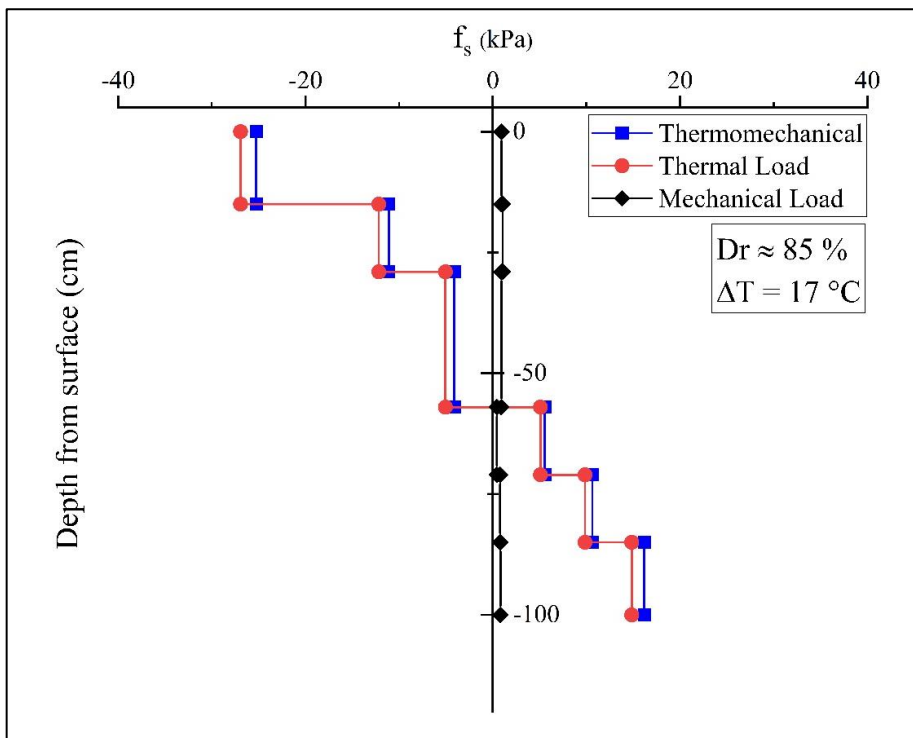
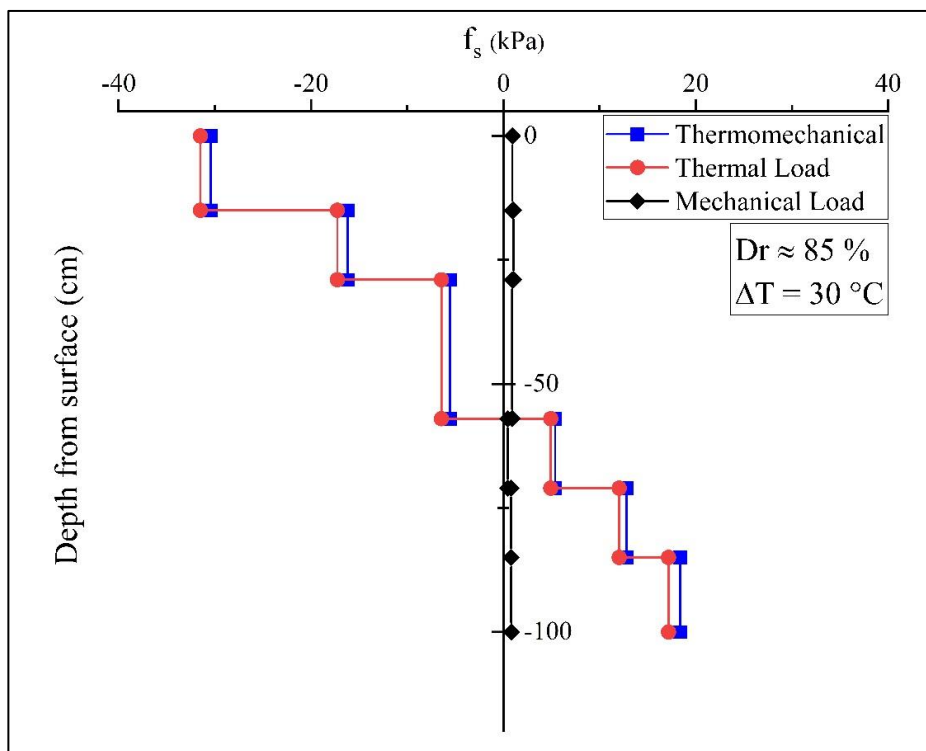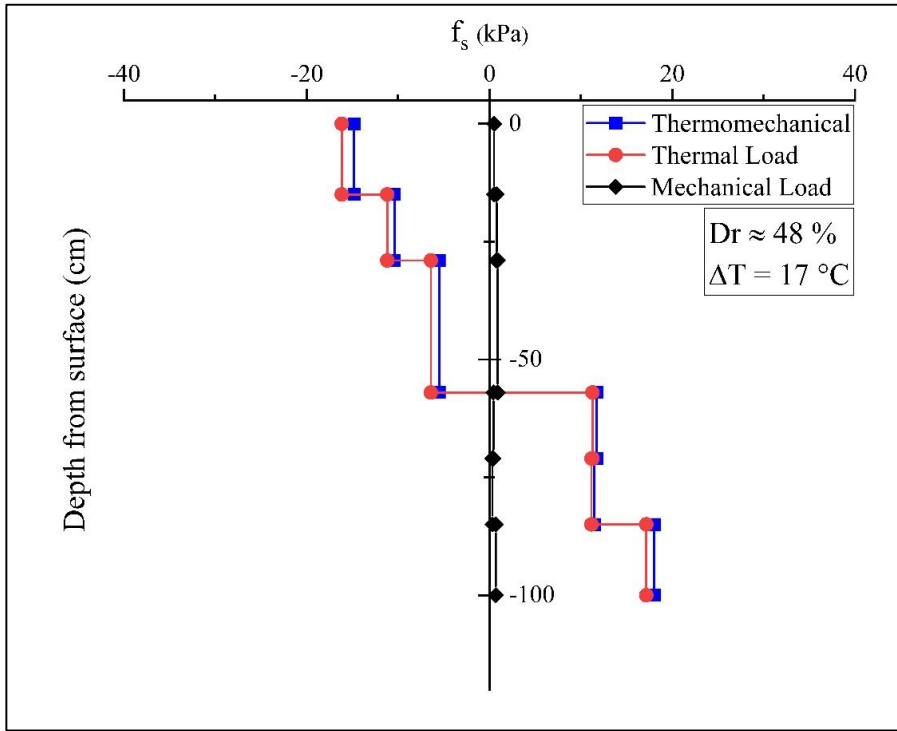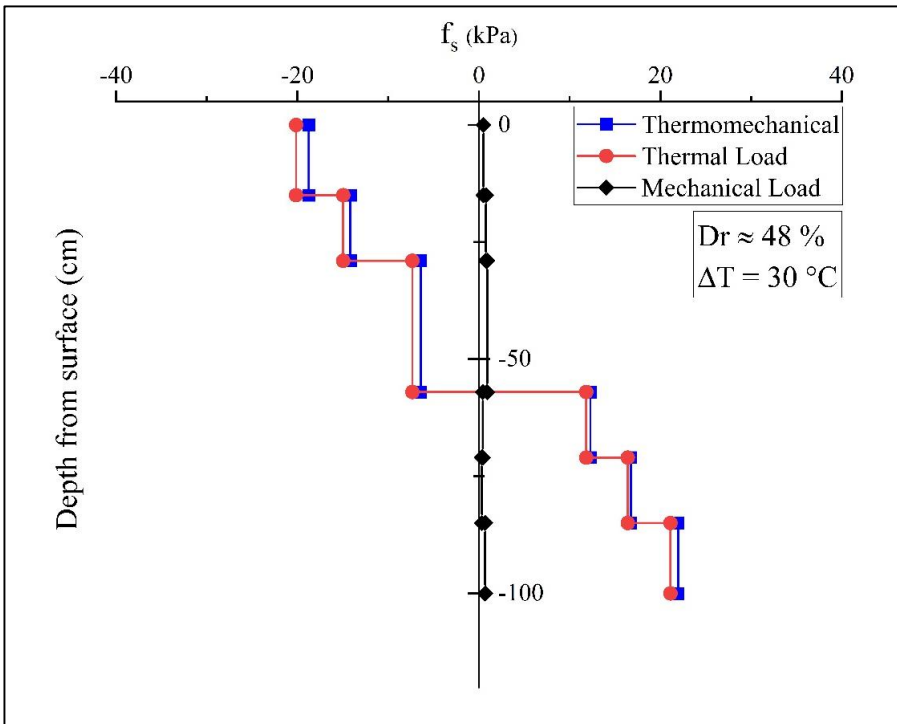**(a)**
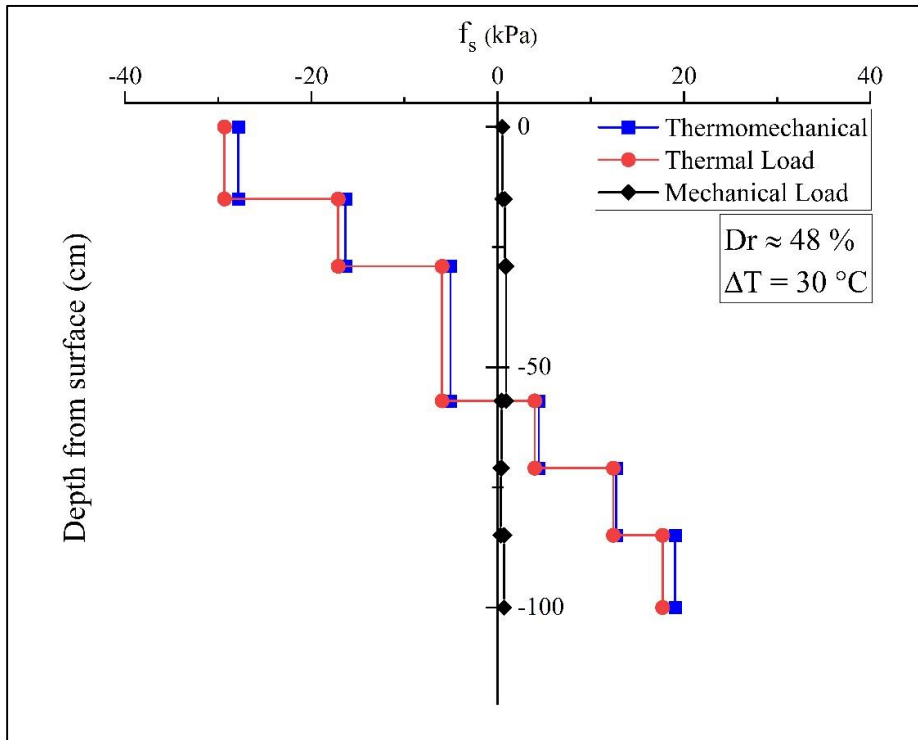
(b)

Fig. 10. Side shear stress along the pile for mechanical, thermal, and thermomechanical loadings in the base-only-restrained condition, (a) Dr ≈ 48%, ΔT=17°C, (b) Dr ≈ 48%, ΔT=30°C, (c) Dr ≈ 85%, ΔT=17°C, and (d) Dr ≈ 85%, ΔT=30°C. (Continued)

(c)

(d)

Fig. 10. Side shear stress along the pile for mechanical, thermal, and thermomechanical loadings in the base-only-restrained condition, (a) Dr ≈ 48%, ΔT=17°C, (b) Dr ≈ 48%, ΔT=30°C, (c) Dr ≈ 85%, ΔT=17°C, and (d) Dr ≈ 85%, ΔT=30°C
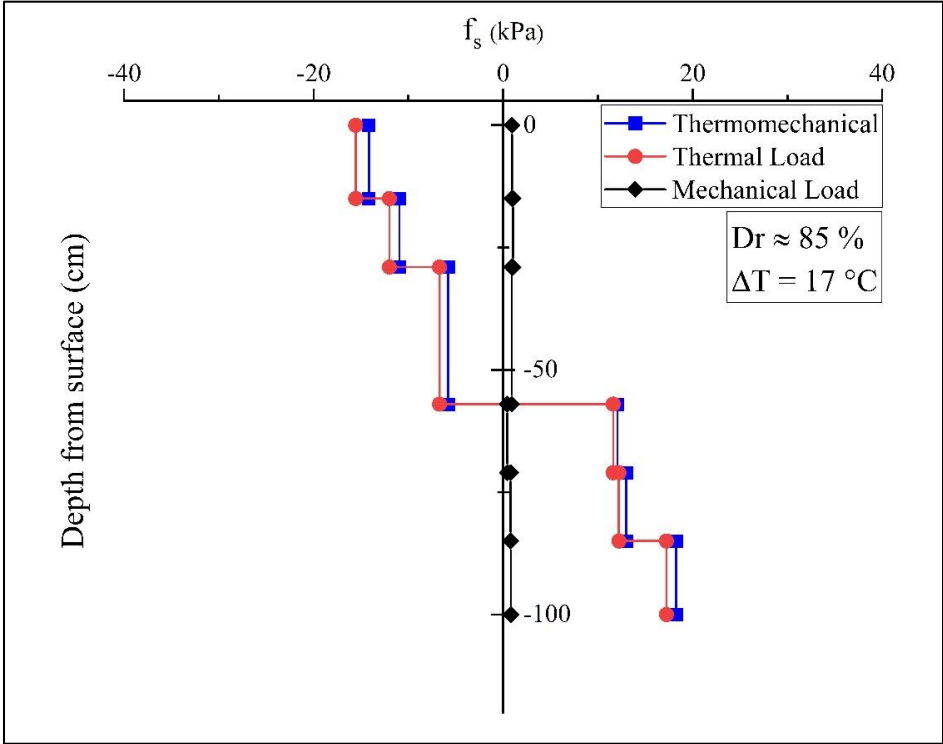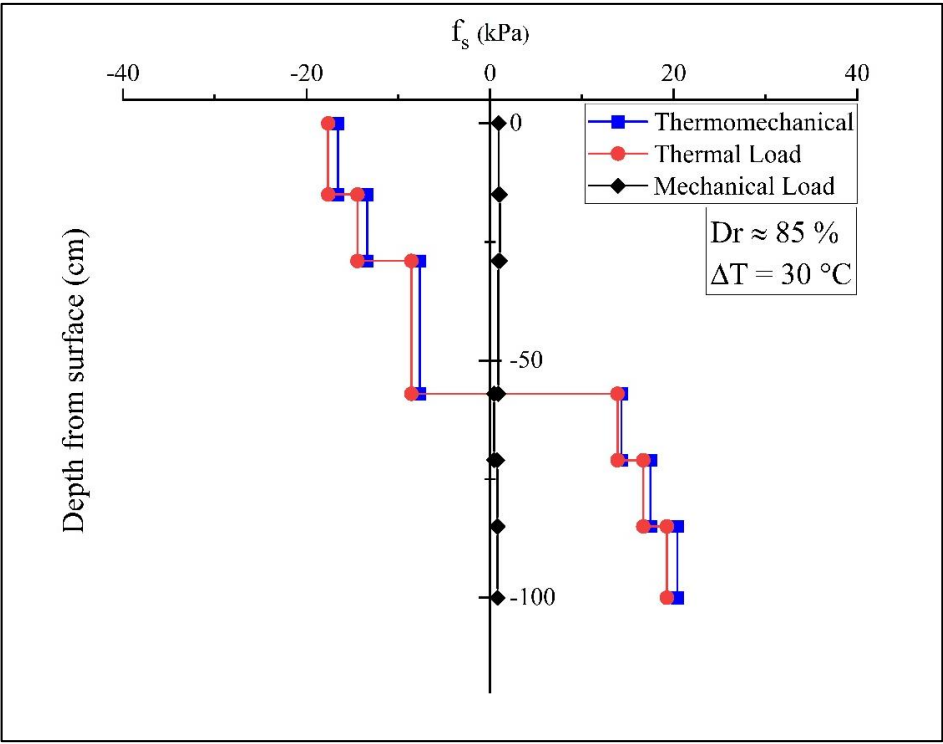
(a)

(b)

Fig. 11. Side shear stress along the pile depth for mechanical, thermal, and thermomechanical loadings in the both-ends-restrained condition: (a) Dr ≈ 48%, ΔT=17°C, (b) Dr ≈ 48%, ΔT=30°C, (c) Dr ≈ 85%, ΔT=17°C, and (d) Dr ≈ 85%, ΔT=30°C. (Continued)

(c)

(d)

Fig. 11. Side shear stress along the pile depth for mechanical, thermal, and thermomechanical loadings in the both-ends-restrained condition: (a) Dr ≈ 48%, ΔT=17°C, (b) Dr ≈ 48%, ΔT=30°C, (c) Dr ≈ 85%, ΔT=17°C, and (d) Dr ≈ 85%, ΔT=30°C.
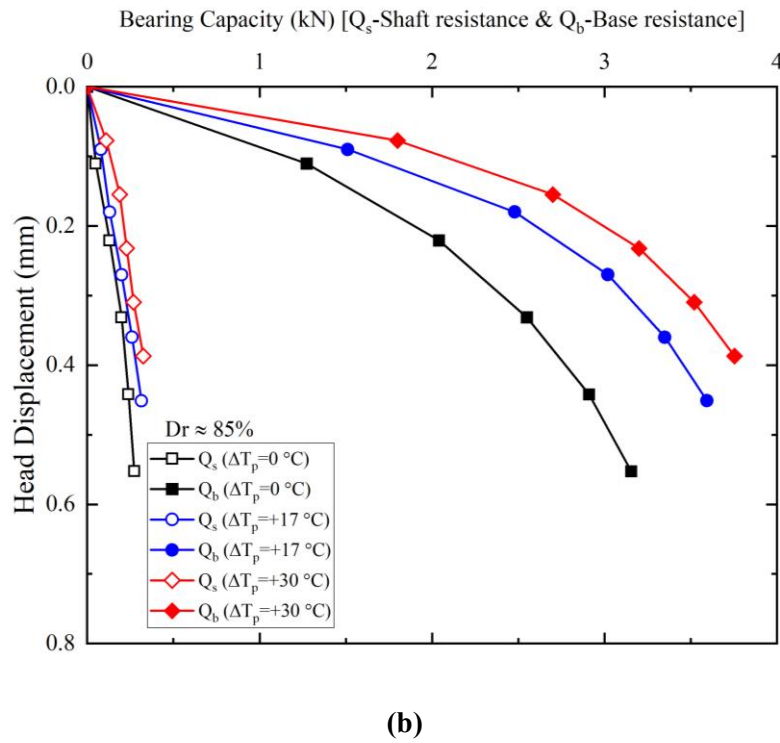
(a)

(b)

Fig. 12. Bearing capacity of the pile (base and shaft resistance) versus pile head settlement for mechanical loading and thermomechanical loading with ΔT=17°C and ΔT=30°C: (a) base-only-restrained condition and Dr = 48%, (b) base-only-restrained condition and Dr = 85%, (c) both-ends-restrained condition and Dr = 48%, and (d) both-ends-restrained condition and Dr = 85%. (Continued)
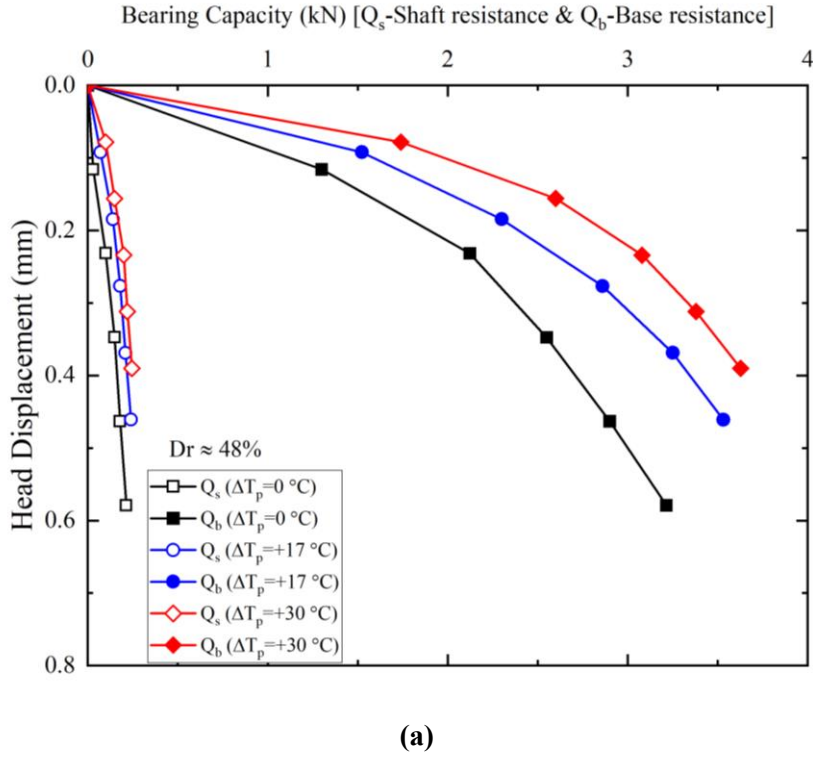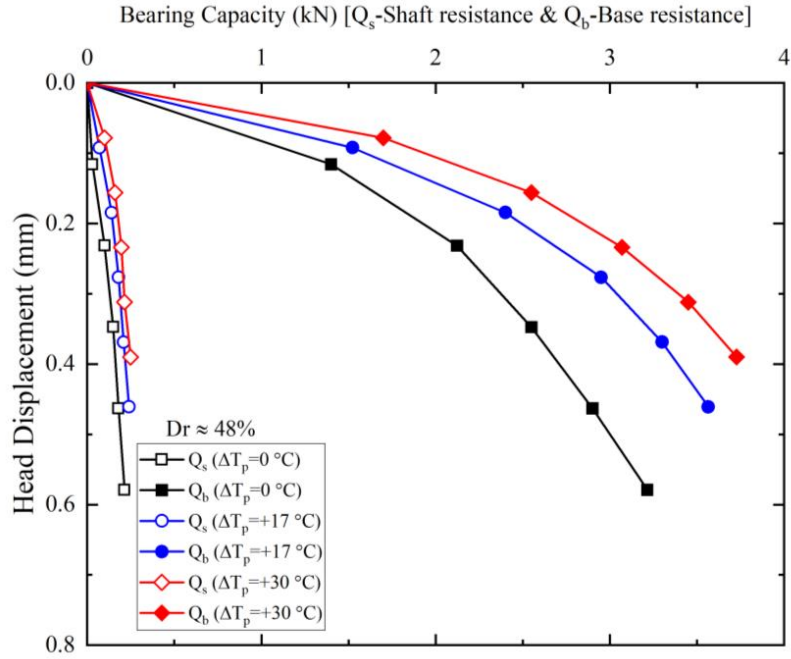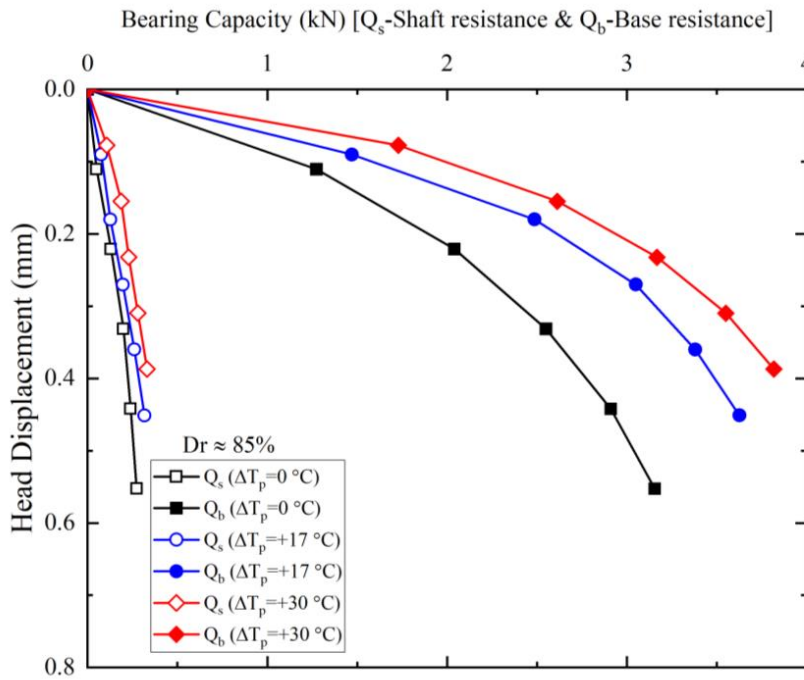
(c)

(d)

Fig. 12. Bearing capacity of the pile (base and shaft resistance) versus pile head settlement for mechanical loading and thermomechanical loading with ΔT=17°C and ΔT=30°C: (a) base-only-restrained condition and Dr = 48%, (b) base-only-restrained condition and Dr = 85%, (c) both-ends-restrained condition and Dr = 48%, and (d) both-ends-restrained condition and Dr = 85%.
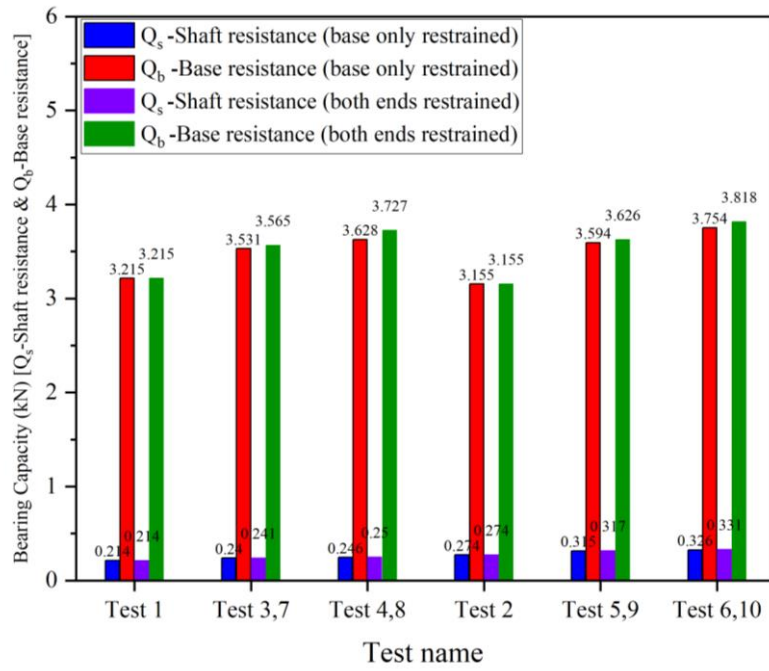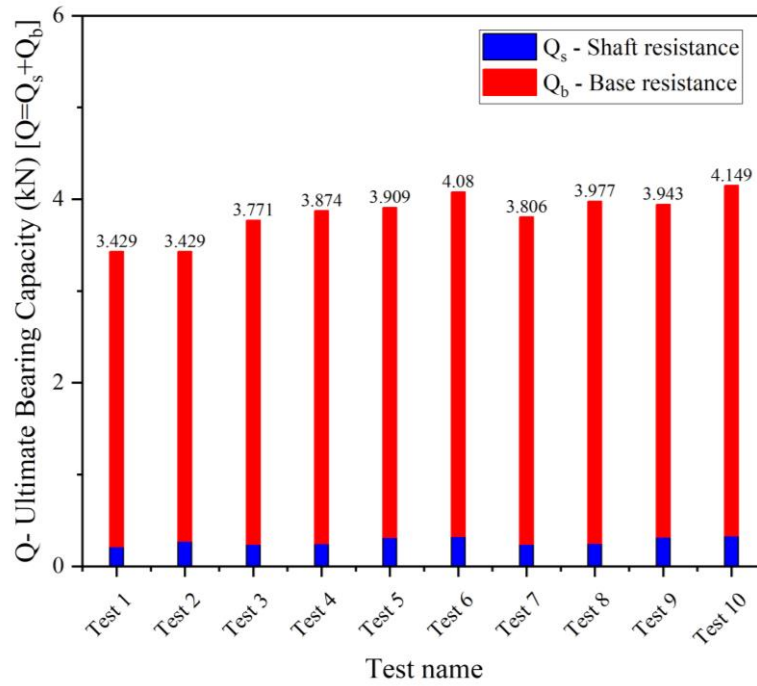
(a)

(b)

Fig. 13. (a) The resistance value of the pile base and shaft in all the tests, (b) The ultimate bearing capacity in all the tests.

Table 3. Summary of ultimate bearing capacities changes for different tests.

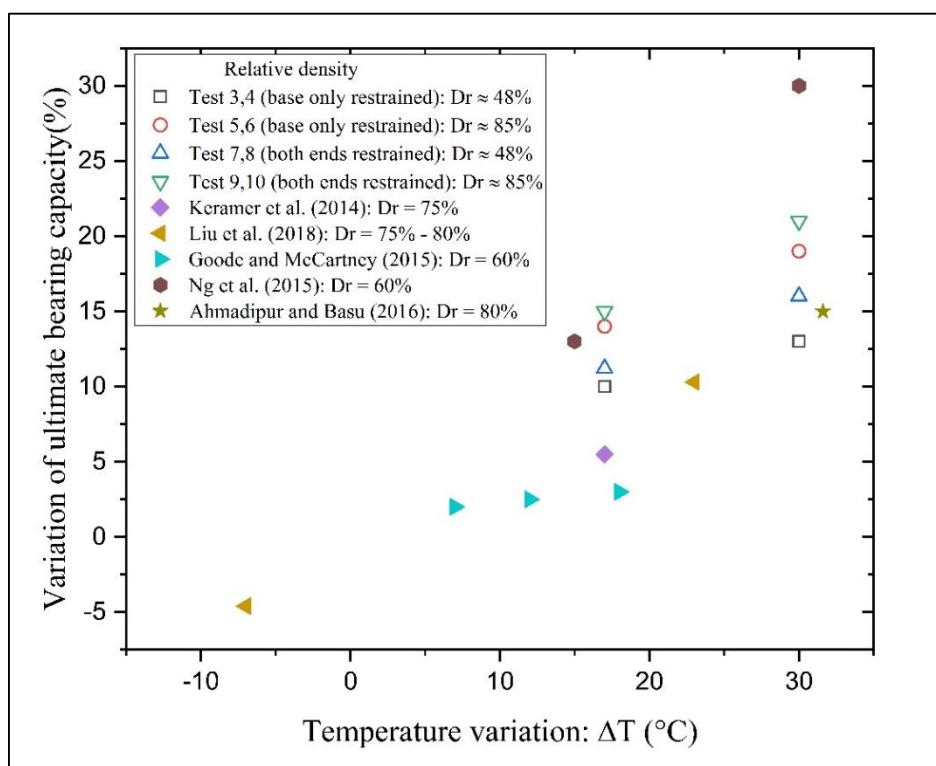|	Test Name	Change in ultimate bearing capacity: %
base only restrained	Test 3	10
	Test 4	13
	Test 5	14
	Test 6	19
both ends restrained	Test 7	11
	Test 8	16
	Test 9	15
	Test 10	21

Fig. 14. Change of ultimate bearing capacity under thermal loading for different studies.

This figure compares the effects of thermal loading obtained from the literature and current study on the ultimate bearing capacity of piles installed in sandy soil. The differences in the results can be because of different boundary conditions, thermal loadings, soil types, various degrees of saturation, etc.

The descriptions of the studies mentioned in Fig. 14 are given below:

Kramer and Basu reported that an increase of 17 °C resulted in an increase of about 5.5% in the bearing capacity of the pile [31]. Liu et al. found that the bearing capacity changed by -4.6% (U-shaped) and 10.3% (W-shaped) when the temperature changed to $\Delta T = -7$ °C and $\Delta T = +23$ °C, respectively [33]. Goode and McCartney reported slight changes in bearing capacity due to an increase of 7 °C, 12 °C, and 18 °C. This was mainly due to the lower relative density and the compaction method used in their study, which could not produce a sufficient change in lateral stress [32]. Ng et al. reported that the bearing capacity of the pile increased by 13% and 30% when the temperature was increased to 15 °C and 30 °C, even though the relative density was not high. They pointed out that their study's high thermal expansion of

the aluminum pile had increased the bearing capacity [28]. Ahmadipour and Basu reported a 15% increase in the bearing capacity when the temperature of the pile was increased to 31.6 °C and showed that the resistance of the wall and the top had increased by 16% and 10%, respectively [43].

5- Conclusion

Utilizing energy piles significantly improves the GSHP system's cost-effectiveness due to the elimination of drilling costs. However, to utilize it, it is essential to address the prevailing uncertainty regarding the thermomechanical characteristics of the energy pile under different conditions. This study helps to better understand the thermomechanical characteristics of piles under multiple conditions. The changes in the ultimate bearing capacity of the pile in the dry Firoozkooh sand with relative densities of 48% and 85% and with $\Delta T=17$ °C and $\Delta T=30$ °C were determined under the two base-only-restrained and both-ends-restrained conditions. In this study, it was found that the pile's grip and end conditions significantly affect the stresses created in the pile, and it is necessary to see this effect completely for real designs. Also, in the case where the pile is sitting at the end on the incompressible bedrock (end-bearing condition), the effect of the relative density of the surrounding soil is reduced compared to the semi-floating condition. The outstanding results of this study are as follows:

- Thermal loading (heating load only) increases the stresses and resistance of the tip and shaft, which also raises the bearing capacity.
- The thermal stresses for the both-ends-restrained condition were greater than those for the base-only-restrained condition. There was an increase of 35% and 28% in the thermal stress for $\Delta T=17$ °C and $\Delta T=30$ °C, respectively, in the both-ends-restrained condition compared to the base-only-restrained condition.
- An increase in relative density led to increased thermal stresses and bearing capacity, but its effect on bearing capacity was far more significant.
- The bearing capacity for the base-only-restrained condition in the relative density of 48% increased by 10% and 13% for $\Delta T=17$ °C and $\Delta T=30$ °C, respectively. Moreover, it increased by 14% and 19% in the relative density of 85% for $\Delta T=17$ °C and $\Delta T=30$ °C, respectively.
- Ultimate bearing capacity for the both-ends-restrained condition in the relative density of 48% increased by 11% and 16%, respectively, when $\Delta T=17$ °C and $\Delta T=30$ °C. The bearing capacity also increased by 15% and 21% in the relative density of 85% when $\Delta T=17$ °C and $\Delta T=30$ °C, respectively.

Recommendation for future research

Future research is needed to explore the behavior of EPs under cooling conditions, cyclic heating and cooling load, dynamic mechanical loading (earthquake loading), and long-term conditions.

Conflicts of Interest: The authors declare that they have no competing interests.

References

[1] D. Ürge-Vorsatz, L. F. Cabeza, S. Serrano, C. Barreneche, and K. Petrichenko, "Heating and cooling energy trends and drivers in buildings," Renewable and Sustainable Energy Reviews, vol. 41, pp. 85-98, 2015/01/01/ 2015, doi: https://doi.org/10.1016/j.rser.2014.08.039, doi: https://doi.org/10.1016/j.rser.2014.08.039.

[2] Y. H. Yau and S. Hasbi, "A review of climate change impacts on commercial buildings and their technical services in the tropics," Renewable and Sustainable Energy Reviews, vol. 18, pp. 430-441, 2013/02/01/ 2013, doi: https://doi.org/10.1016/j.rser.2012.10.035, doi: https://doi.org/10.1016/j.rser.2012.10.035.

[3] O. Ghasemi-Fare and P. Basu, "Predictive assessment of heat exchange performance of geothermal piles," Renewable energy, vol. 86, pp. 1178-1196, 2016.

[4] H. Brandl, "Energy foundations and other thermo-active ground structures," Géotechnique, vol. 56, no. 2, pp. 81-122, 2006.

[5] T. Amis, P. Bourne-Webb, C. Davidson, B. Amatya, and K. Soga, "The effects of heating and cooling energy piles under working load at Lambeth College, UK," in Proceedings of the 33rd Annual and 11th International Conference on Deep Foundations, 2008, p. 10.

[6] O. Boënnec, "Piling on the energy," Geodrilling International, vol. 150, pp. 25-28, 2009.

[7] J. S. McCartney, D. LaHaise, T. LaHaise, and J. Rosenberg, "Application of geoexchange experience to geothermal foundations," in Art of Foundation Engineering Practice, 2010, pp. 411-422.

[8] A. Akbari Garakani, B. Heidari, S. Mokhtari Jozani, and O. Ghasemi-Fare, "Numerical and Analytical Study on Axial Ultimate Bearing Capacity of Fixed-Head Energy Piles in Different Soils," International Journal of Geomechanics, vol. 22, no. 1, p. 04021258, 2022, doi: https://doi.org/10.1061/(ASCE)GM.1943-5622.0002223, doi: https://doi.org/10.1061/(ASCE) GM.1943-5622.0002223.

[9] D. Y. Cherati and O. Ghasemi-Fare, "Practical approaches for implementation of energy piles in Iran based on the lessons learned from the developed countries experiences," Renewable and Sustainable Energy Reviews, vol. 140, p. 110748, 2021.

[10] D. Y. Cherati and O. Ghasemi-Fare, "Analyzing transient heat and moisture transport surrounding a heat source in unsaturated porous media using the Green's function," Geothermics, vol. 81, pp. 224-234, 2019/09/01/ 2019, doi: https://doi.org/10.1016/j.geothermics.2019.04.012, doi: https://doi.org/10.1016/j.geothermics.2019.04.012.

[11] S. G. Alpaydin and Y. Yukselen-Aksoy, "Investigation of shear strength of sand–bentonite mixtures with boron additives at high temperature for energy geo-structures," Environmental Earth Sciences, vol. 82, no. 10, p. 256, 2023/05/15 2023, doi: 10.1007/s12665-023-10972-6, doi: 10.1007/s12665-023-10972-6.

[12] R. Saggu and T. Chakraborty, "Thermal analysis of energy piles in sand," Geomechanics and Geoengineering, vol. 10, no. 1, pp. 10-29, 2015/01/02 2015, doi: 10.1080/17486025.2014.923586, doi:

10.1080/17486025.2014.923586.

[13] O. Ghasemi-Fare et al., "A Feasibility Study of Bridge Deck Deicing Using Geothermal Energy," (in English), Tech Report 2015. [Online]. Available: https://rosap.ntl. bts.gov/view/dot/29032,

[14] M. Faizal, A. Bouazza, C. Haberfield, and J. S. McCartney, "Axial and radial thermal responses of a field-scale energy pile under monotonic and cyclic temperature changes," Journal of Geotechnical and Geoenvironmental Engineering, vol. 144, no. 10, p. 04018072, 2018, doi: https://doi.org/10.1061/(ASCE) GT.1943-5606.0001952, doi: https://doi.org/10.1061/ (ASCE)GT.1943-5606.0001952.

[15] J. Fang, G. Kong, Y. Meng, L. Wang, and Q. Yang, "Thermomechanical Behavior of Energy Piles and Interactions within Energy Pile–Raft Foundations," Journal of Geotechnical and Geoenvironmental Engineering, vol. 146, no. 9, p. 04020079, 2020/09/01 2020, doi: 10.1061/(ASCE)GT.1943-5606.0002333, doi: 10.1061/(ASCE)GT.1943-5606.0002333.

[16] L. Laloui and M. Sutman, "Experimental investigation of energy piles: From laboratory to field testing," Geomechanics for Energy and the Environment, vol. 27, p. 100214, 2021/09/01/ 2021, doi: https:// doi.org/10.1016/j.gete.2020.100214, doi: https://doi. org/10.1016/j.gete.2020.100214.

[17] Y. Zhou, G. Kong, and Q. Yang, "Field performances of energy pile based on the secondary utilization of sonic logging pipes," Geomechanics for Energy and the Environment, vol. 32, p. 100280, 2022/12/01/ 2022, doi: https://doi.org/10.1016/j.gete.2021.100280, doi: https:// doi.org/10.1016/j.gete.2021.100280.

[18] J. Luo, H. Zhao, W. Huang, Y. Zhu, W. Xiang, and J. Rohn, "Determination of ground thermal properties for energy piles by thermal response tests," Environmental Earth Sciences, vol. 77, no. 4, p. 152, 2018/02/19 2018, doi: 10.1007/s12665-018-7265-1, doi: 10.1007/s12665-018-7265-1.

[19] Y. Guo, C. Wang, A. Bouazza, H. Chang, and G. Kong, "Thermal performance of a full-scale pre-tensioned high strength concrete (PHC) energy pile," Journal of Energy Storage, vol. 98, p. 112840, 2024/09/15/ 2024, doi: https://doi.org/10.1016/j.est.2024.112840, doi: https:// doi.org/10.1016/j.est.2024.112840.

[20] T. Wang, H. Liu, G. Kong, C. Wang, and X. Hu, "Field test on thermal control for bridge piers on plateau through energy pile," Renewable Energy, vol. 230, p. 120896, 2024/09/01/ 2024, doi: https://doi.org/10.1016/j. renene.2024.120896, doi: https://doi.org/10.1016/j. renene.2024.120896.

[21] M. Faizal, A. Bouazza, J. S. McCartney, and C. Haberfield, "Axial and radial thermal responses of energy pile under six storey residential building," Canadian Geotechnical Journal, vol. 56, no. 7, pp. 1019-1033, 2019, doi: https://doi.org/10.1139/cgj-2018-0246, doi: https://doi.org/10.1139/cgj-2018-0246.

[22] F. Loveridge, J. S. McCartney, G. A. Narsilio, and M. Sanchez, "Energy geostructures: a review of analysis approaches, in situ testing and model scale experiments," Geomechanics for Energy and the Environment, vol. 22,

p. 100173, 2020.

[23] R. P. Cunha and P. J. Bourne-Webb, "A critical review on the current knowledge of geothermal energy piles to sustainably climatize buildings," Renewable and Sustainable Energy Reviews, vol. 158, p. 112072, 2022/04/01/ 2022, doi: https://doi.org/10.1016/j. rser.2022.112072, doi: https://doi.org/10.1016/j. rser.2022.112072.

[24] Z. Mohamad, F. Fardoun, and F. Meftah, "A review on energy piles design, evaluation, and optimization," Journal of Cleaner Production, vol. 292, p. 125802, 2021/04/10/ 2021, doi: https://doi.org/10.1016/j. jclepro.2021.125802, doi: https://doi.org/10.1016/j. jclepro.2021.125802.

[25] J. S. McCartney and J. E. Rosenberg, "Impact of heat exchange on side shear in thermo-active foundations," presented at the Geo-frontiers 2011: Advances in geotechnical engineering, 2011.

[26] D. Wu, H. Liu, G. Kong, and C. Li, "Thermo-mechanical behavior of energy pile under different climatic conditions," Acta Geotechnica, vol. 14, no. 5, pp. 1495-1508, 2019/10/01 2019, doi: 10.1007/s11440-018-0731-9, doi: 10.1007/s11440-018-0731-9.

[27] C. Pasten and J. C. Santamarina, "Thermally Induced Long-Term Displacement of Thermoactive Piles," Journal of Geotechnical and Geoenvironmental Engineering, vol. 140, no. 5, p. 06014003, 2014/05/01 2014, doi: 10.1061/ (ASCE)GT.1943-5606.0001092, doi: 10.1061/(ASCE) GT.1943-5606.0001092.

[28] C. W. W. Ng, C. Shi, A. Gunawan, L. Laloui, and H. Liu, "Centrifuge modelling of heating effects on energy pile performance in saturated sand," Canadian Geotechnical Journal, vol. 52, no. 8, pp. 1045-1057, 2015, doi: https://doi.org/10.1139/cgj-2014-030, doi: https://doi. org/10.1139/cgj-2014-030.

[29] P. B. Omid Ghasemi-Fare "Influences of ground saturation and thermal boundary condition on energy harvesting using geothermal piles," Energy & Buildings 2018, doi: https://doi.org/10.1016/j.enbuild.2018.01.030

[30] A. Moshfegh, A. Abouei Mehrizi, A. Javadzadegan, M. Joshaghani, and O. Ghasemi-Fare, "Numerical investigation of various nanofluid heat transfers in microchannel under the effect of partial magnetic field: lattice Boltzmann approach," Journal of Thermal Analysis and Calorimetry, vol. 140, no. 2, pp. 773-787, 2020/04/01 2020, doi: 10.1007/s10973-019-08862-w, doi: 10.1007/s10973-019-08862-w.

[31] C. Kramer and P. Basu, "Performance of a model geothermal pile in sand," in Proc. 8th Int. Conf. on Physical Modelling in Geotechnics, Perth (Gaudin, C. & White, D.(eds)). Leiden: CRC Press/Balkema, 2014, pp. 771-777.

[32] J. Goode Iii and J. S. McCartney, "Centrifuge modeling of end-restraint effects in energy foundations," Journal of Geotechnical and Geoenvironmental Engineering, vol. 141, no. 8, p. 04015034, 2015.

[33] H.-l. Liu, C.-l. Wang, G.-q. Kong, and A. Bouazza, "Ultimate bearing capacity of energy piles in dry and saturated sand," Acta Geotechnica, vol. 14, no. 3, pp.

869-879, 2019.

[34] M. Sutman, G. Olgun, L. Laloui, and T. Brettmann, "Effect of end-restraint conditions on energy pile behavior," in Geotechnical Frontiers 2017, 2017, pp. 165-174.

[35] M. Sutman, T. Brettmann, and C. G. Olgun, "Full-scale in-situ tests on energy piles: Head and base-restraining effects on the structural behaviour of three energy piles," Geomechanics for Energy and the Environment, vol. 18, pp. 56-68, 2019/06/01/ 2019, doi: https://doi.org/10.1016/j.gete.2018.08.002, doi: https://doi.org/10.1016/j.gete.2018.08.002.

[36] H. H. Senejani, O. Ghasemi-Fare, D. Y. Cherati, and F. Jafarzadeh, "Investigation of thermo-mechanical response of a geothermal pile through a small-scale physical modelling," in E3S Web of Conferences, 2020, vol. 205: EDP Sciences, p. 05016, doi: https://doi.org/10.1051/e3sconf/202020505016.

[37] M. Moshtaghi, M. Keramati, O. Ghasemi-Fare, A. Pourdeilami, and M. Ebrahimi, "Experimental study on thermomechanical behavior of energy piles in sands with different relative densities," Journal of Cleaner Production, vol. 403, p. 136867, 2023/06/01/ 2023, doi: https://doi.org/10.1016/j.jclepro.2023.136867, doi: https://doi.org/10.1016/j.jclepro.2023.136867.

[38] A. Ghezellou, M. Keramati, and O. Ghasemi-Fare, "Thermomechanical response of energy piles in dry sand under monotonic cooling with varying end-support conditions," Journal of Energy Storage, vol. 82, p. 110469, 2024/03/30/ 2024, doi: https://doi.org/10.1016/j.est.2024.110469, doi: https://doi.org/10.1016/j.est.2024.110469.

[39] R. Hoseinpour, M. Keramati, and C. de Hollanda Cavalcanti Tsuha, "Effect of the Addition of a Second Helix on the Helical Pile Performance in Sand," International Journal of Civil Engineering, 2023/09/14 2023, doi: 10.1007/s40999-023-00893-7, doi: 10.1007/s40999-023-00893-7.

[40] S. S. Hosseini, M. Keramati, and R. Hoseinpour, "Laboratory Investigation of behavior of Helical piles under monotonic loading at different loading speeds," Sharif Journal of Civil Engineering, 2025. Sharif University of Technology,

[41] M. Moshtaghi, "Investigation of the performance of Energy pile in soil with different relative density by laboratory modeling," M.Sc. Thesis in Geotechnical Engineering, Civil engineering, Shahrood University of Technology, 2022.

[42] M. Moshtaghi and M. Keramati, "Investigating the behavior and system's power output of a model semi-floating energy pile in dry sand," presented at the 2nd International Conference on Earthquake and Seismic Geotechnical, Tabriz, 2023.

[43] A. Ahmadipur and P. Basu, "Temperature-Induced Alterations of the Shaft and Base Resistances of a Model Geothermal Pile in Dry Sand," in Geo-Chicago 2016, 2016, pp. 155-165.

[44] B. Amatya, K. Soga, P. Bourne-Webb, T. Amis, and L. Laloui, "Thermo-mechanical behaviour of energy piles," Géotechnique, vol. 62, no. 6, pp. 503-519, 2012.

[45] K. D. Murphy, J. S. McCartney, and K. S. Henry, "Evaluation of thermo-mechanical and thermal behavior of full-scale energy foundations," Acta Geotechnica, vol. 10, no. 2, pp. 179-195, 2015.

[46] C. Knellwolf, H. Peron, and L. Laloui, "Geotechnical analysis of heat exchanger piles," Journal of Geotechnical and Geoenvironmental Engineering, vol. 137, no. 10, pp. 890-902, 2011.

[47] S. Baycan et al., "Field investigation of a geothermal energy pile: initial observations," in Proceedings of the 18th international conference on soil mechanics and geotechnical engineering, Paris, France, 2013, pp. 2-6.